Introduction to Nanotechnology and Nanoscience – Class#8

Liwei Lin

Professor, Dept. of Mechanical Engineering
Co-Director, Berkeley Sensor and Actuator Center
The University of California, Berkeley, CA94720
e-mail: lwlin@me.berkeley.edu
http://www.me.berkeley.edu/~lwlin

Outline

- Review
- CNT Fabrication Methods
- CNT Resonator
- HW#3
- Paper #2

https://www.nature.com/articles/s41541-020-0159-8

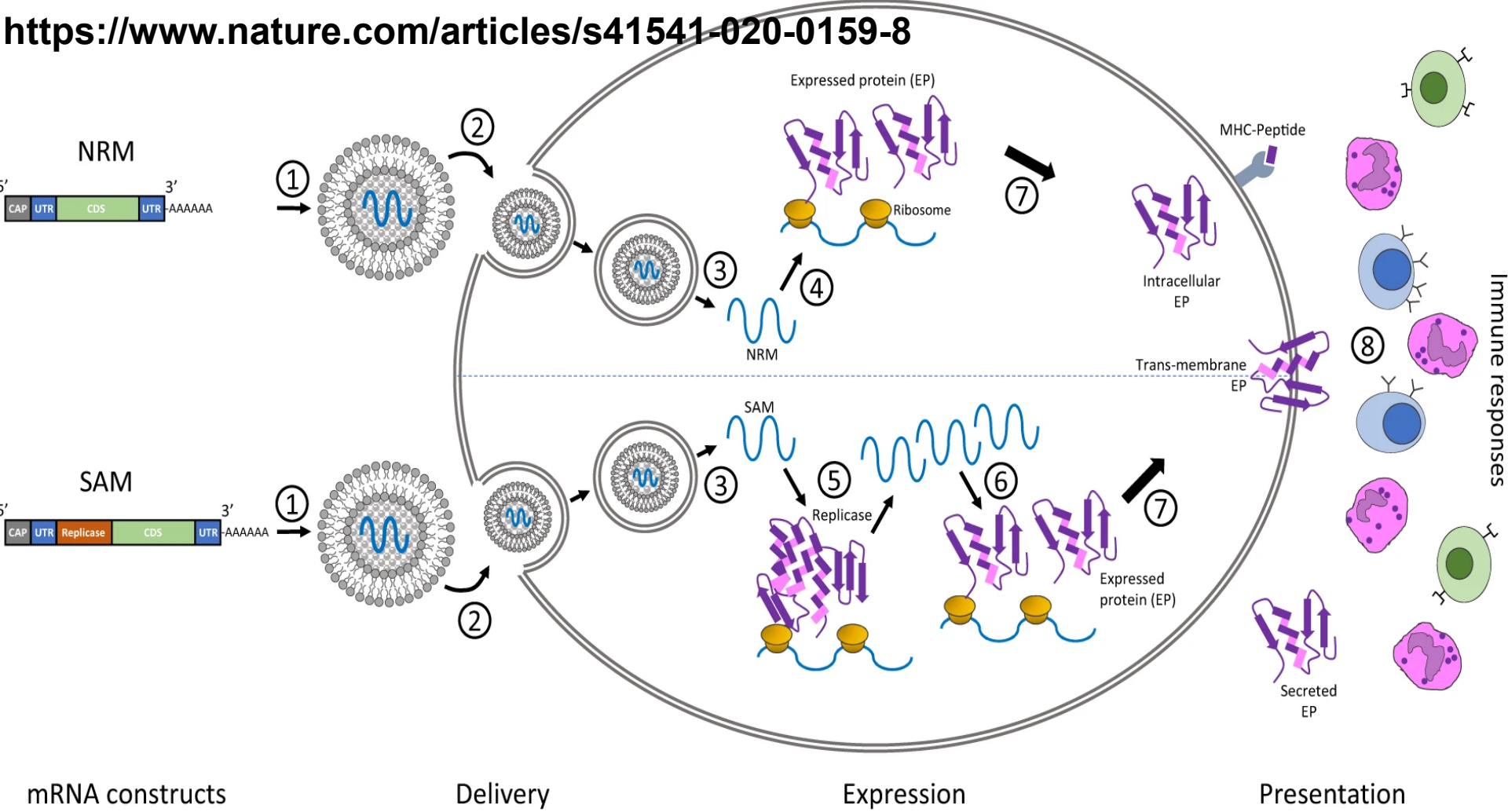

(1) mRNA formulated in lipid nanoparticles (LNPs). (2) Cellular uptake. (3) release of the mRNA into the cytosol. (4) translated by ribosomes to produce the protein of interest. (5) translated by ribosomes to produce the replicase machinery for self-amplification of the mRNA. (6) Self-amplified mRNA to produce the protein of interest. (7) The expressed proteins of interest are generated. (8) The innate and adaptive immune responses detect the protein.

Moderna's mRNA Vaccine Approach

Closely mimics a native viral infection leading to B and T cell responses

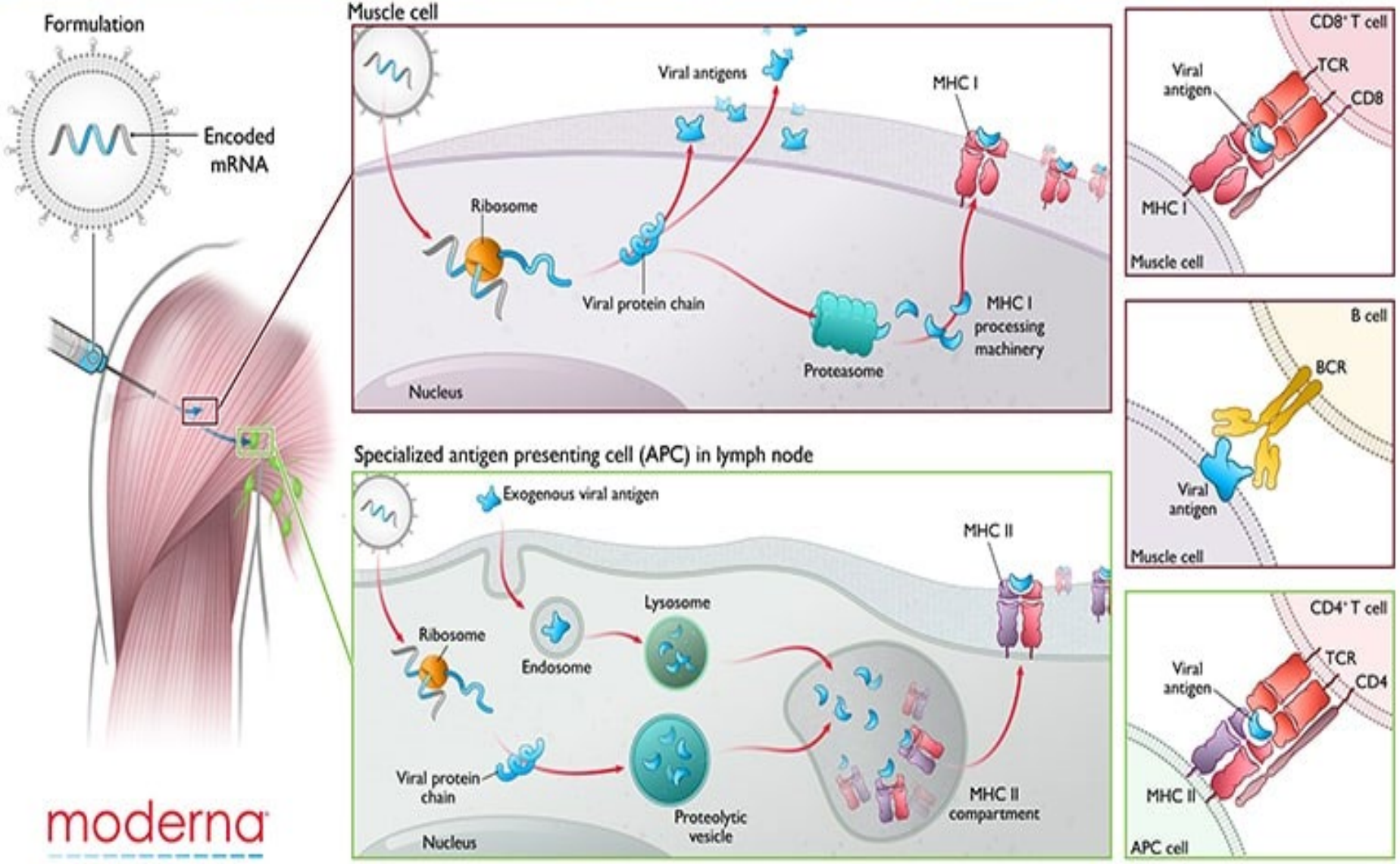

moderna

© 2017 Moderna Therapeutics

COMMENTARY

https://www.wbur.org/commonhealth/2021/02/12/brutal-science-system-mrna-pioneer

How Our Brutal Science System Almost Cost Us A Pioneer Of mRNA Vaccines

February 12, 2021 | By Dr. David Scales

From the photo album of author David Scales (second from right), the 2001 lab team that included Katalin Karikó (third from left.)

Still, Karikó was struggling. Her science was fantastic, but she was less adept at the competitive game of science. She tried again and again to win grants, and each time, her applications were rejected.

Eventually, in the mid-1990s, she suffered the academic indignity of demotion, meaning she was taken off the academic ladder that leads to becoming a professor. We never discussed it personally because by the time I joined the

2023 Nobel Prize in Medicine

Carbon Nanotubes

- Carbon nanotubes belong to a class of molecules known as *fullerenes*
- Fullerenes are a family of highly-symmetrical carbon cage molecules whose prototypical member is C_{60}

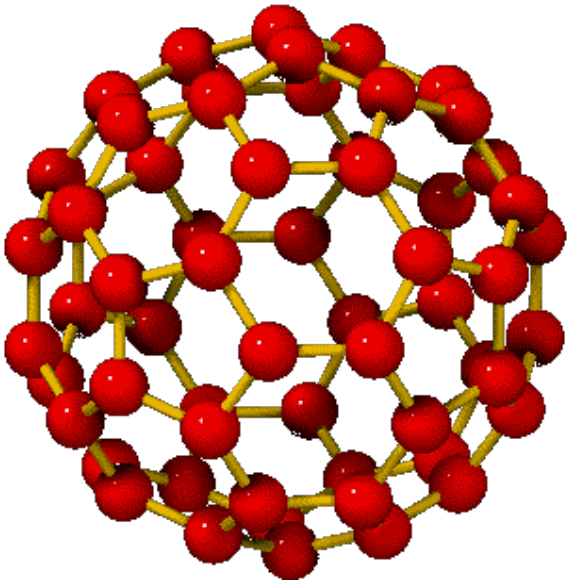

- Discovered by R. Smalley, R. Curl, and H. Kroto
- Nobel Chemistry Prize 1996
- Known as "Buckminster Fullerene" or "Bucky Ball"

How a Carbon Nanotube Differs from a Bucky Ball

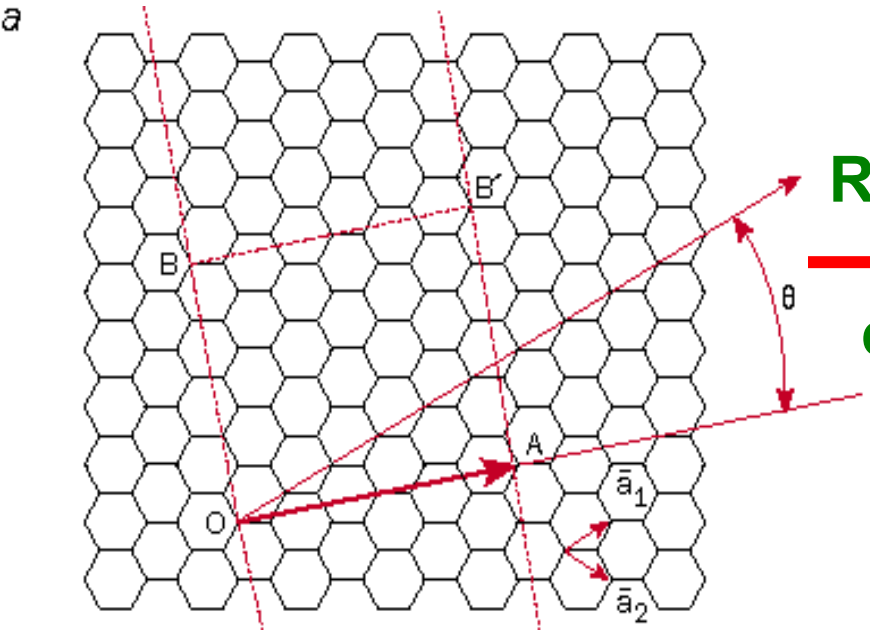

Roll into a cylinder

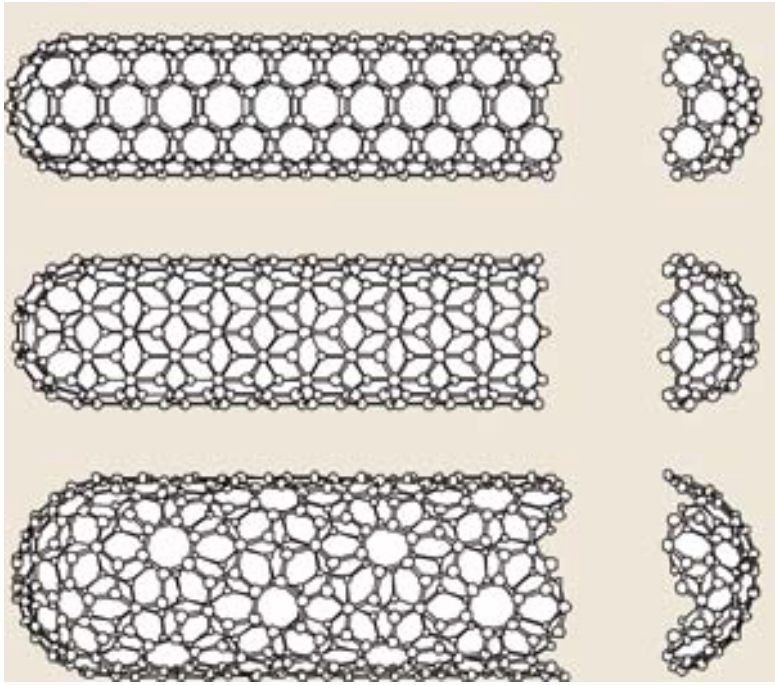

Graphene Sheet

3 Different Nanotubes

Discovered by S. Iijiima (NEC) in 1991

Three Different Types of Carbon Nanotubes

Metallic

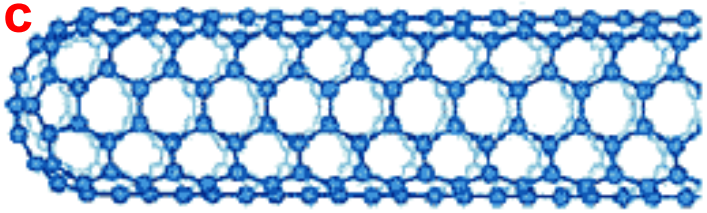

Armchair ($\alpha = 30°$)

Semiconducting/Metallic

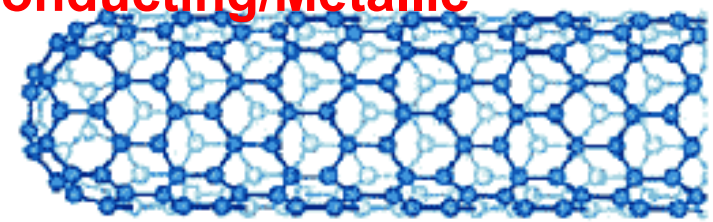

Zigzag ($\alpha = 0°$)

Semiconducting
Semimetallic

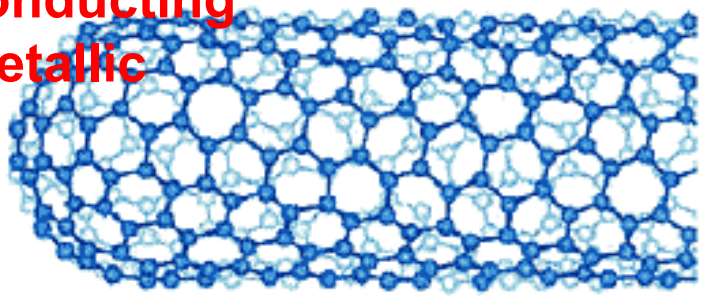

Intermediate ($0 < \alpha < 30°$)

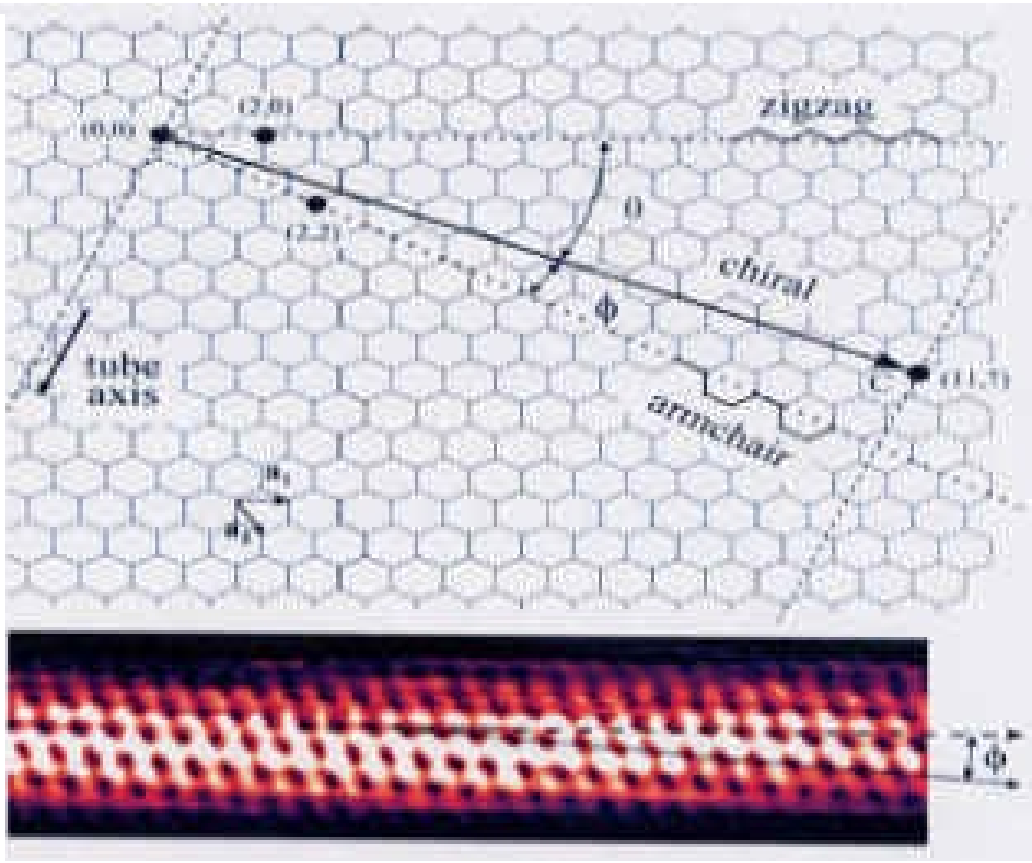

No way to control which way the CNT will "roll"

http://www.applied-nanotech.com/cntproperties.htm

Single or Multi-Walled Carbon Nanotubes

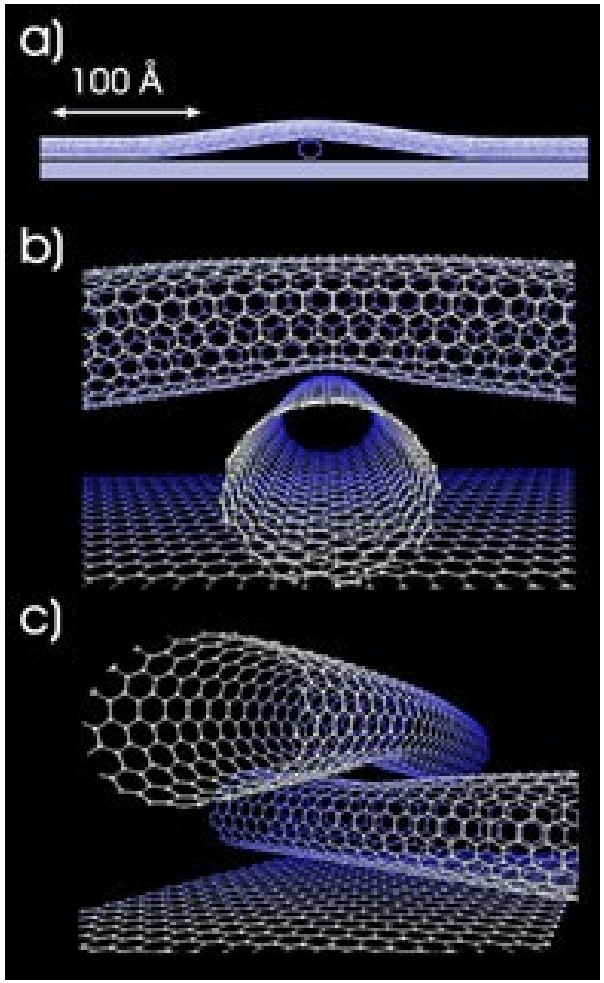

Single-Walled Nanotube
(SWNT)

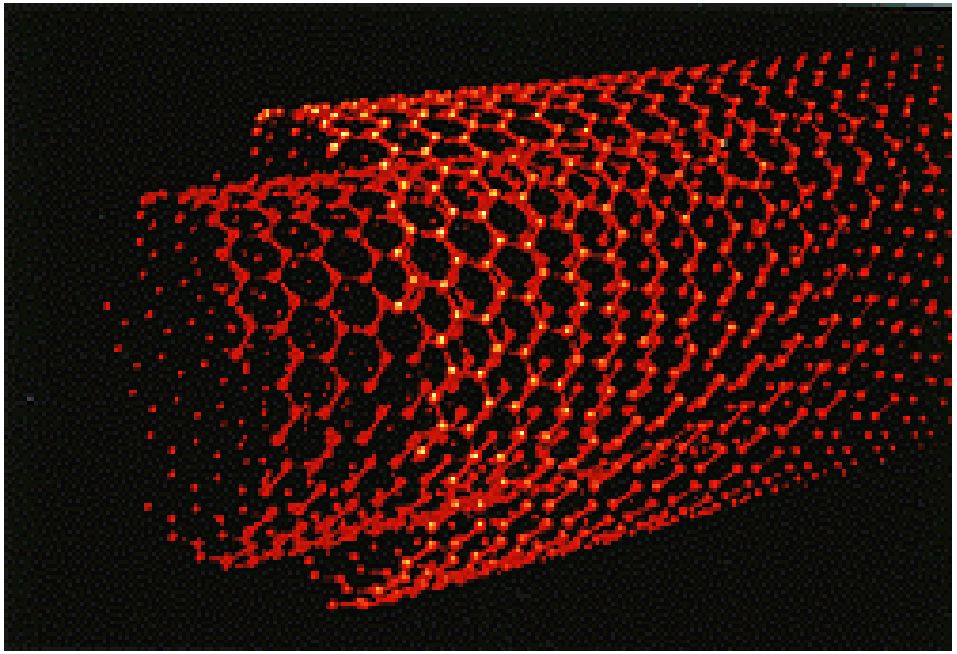

Multi-Walled Nanotube
(MWNT)

SEM Photos of Carbon Nanotubes

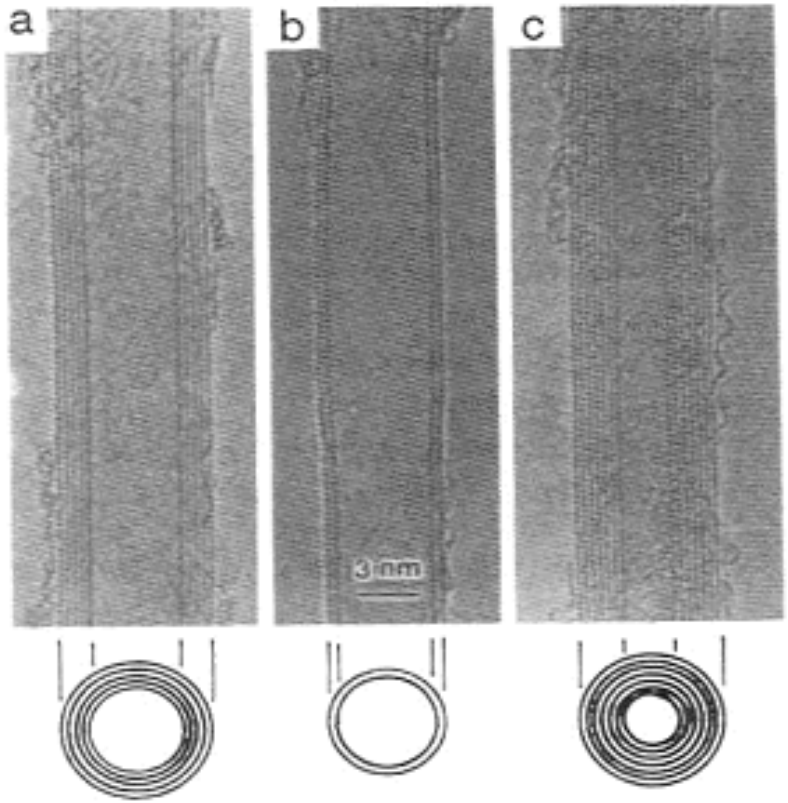

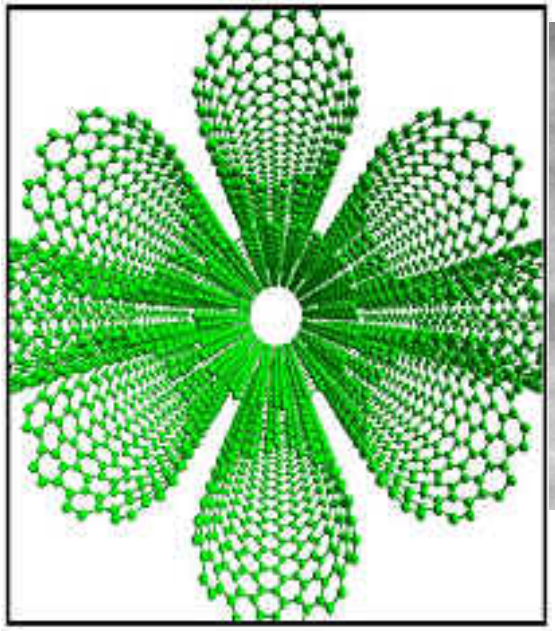

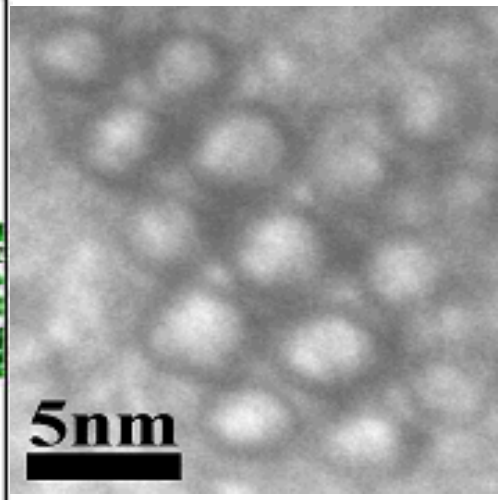

Bundle of SWNT

MWNT
S. Iijima, Nature 1991

How Do You Make Carbon Nanotubes?

- First look at how Bucky balls, C60, are made

— vaporize carbon disc into a high-density helium flow using Nd/YAG laser (which produces 5 ns pulses)

— resulting carbon clusters are expanded in a supersonic molecular beam, photoionized using an excimer beam, and detected via time-of-flight mass spec.

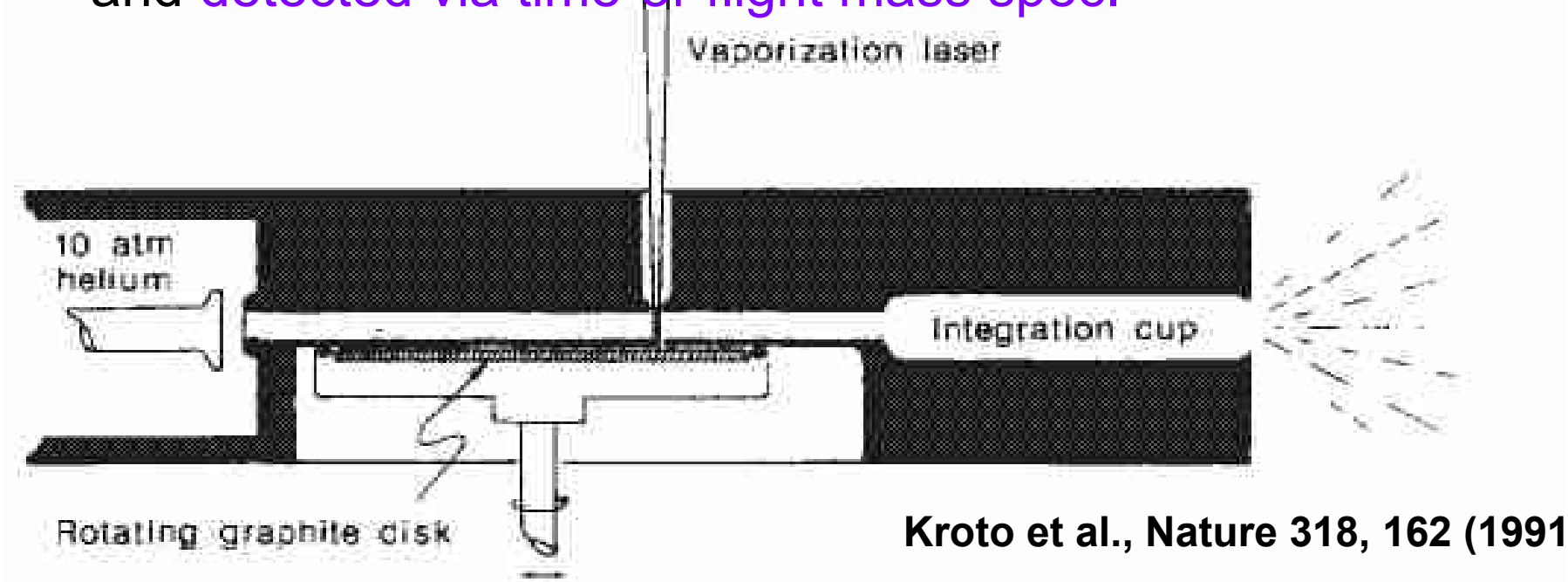

Kroto et al., Nature 318, 162 (1991)

Some Noteworthy Details in C60 Creation

- Graphite disc rotates to provide a smooth vaporization surface
- Helium cools carbon and allows it to react and cluster
- Ionization needed to detect via mass spec. (can get other carbon species and this is why you need mass spec)
- C60 is highly stable

Carbon Nanotube Creation

- Use a **DC arc discharge** in argon and catalyst
- **Nanotubes grow at the negative end** of the electrode
- Can grow nanotubes that are **1-30 nm in diameter and are microns long**
- Nanotubes created are usually **MWNTs**

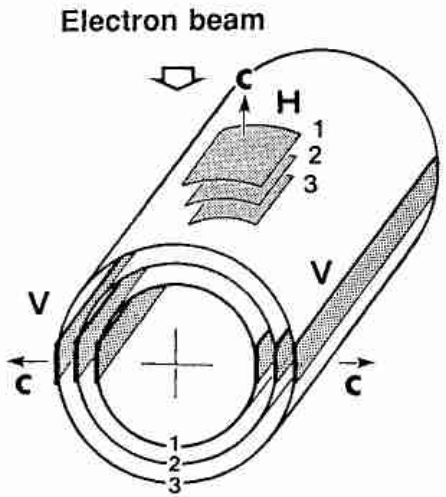

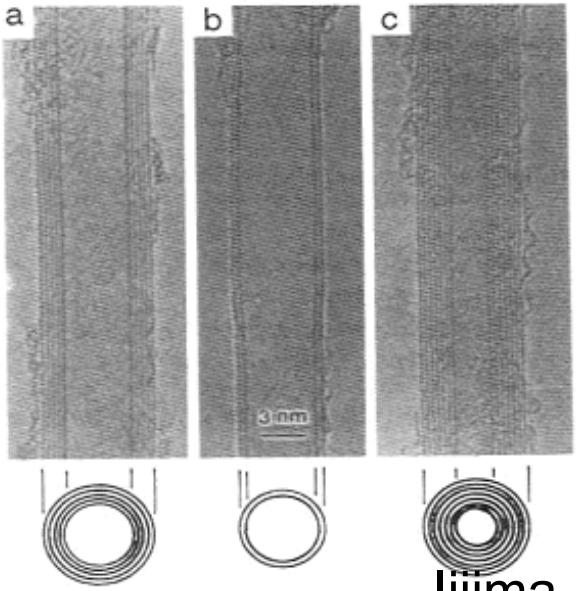

Iijima, Nature 354, 56 (1991)

SWNTs – Pulsed Laser

Pulsed laser ablation

— Ar flows in a 25 mm tube inside a 56 mm tube and everything is heated to 1473 K in a tube furnace

— A composite ablation target is located in front of the 25 mm inner tube and consists of **Ni and Co uniformly mixed with graphite**

— **Ni and Co are catalyst** from which **carbon atoms attach and grow outward**

— Can have contaminants and also van der Waals lead to ropes

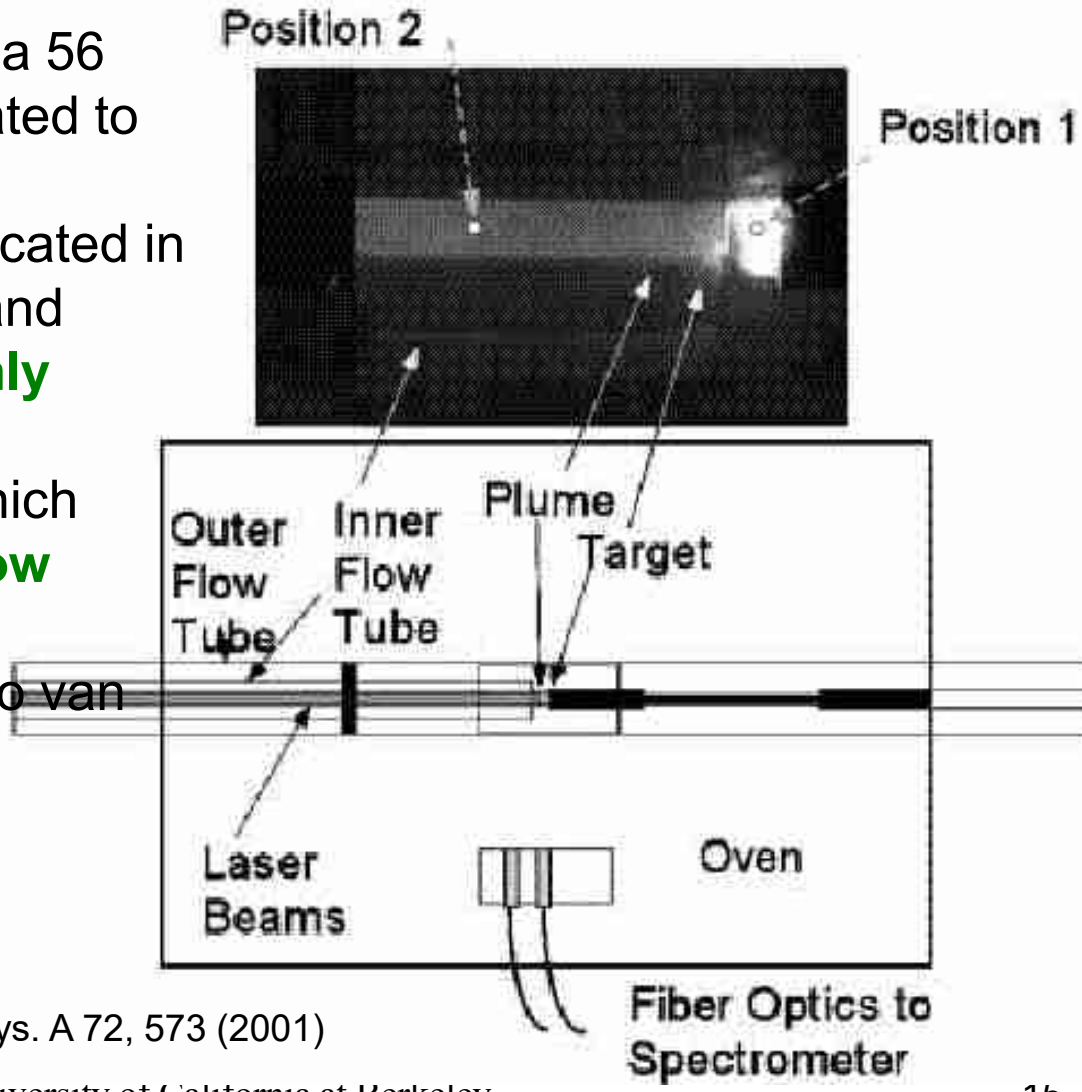

Scott et al., Appl. Phys. A 72, 573 (2001)

SWNTs - CVD

- Can also use chemical vapor deposition (CVD) and nanoparticles such as Fe
- Include water vapor to promote catalytic activity

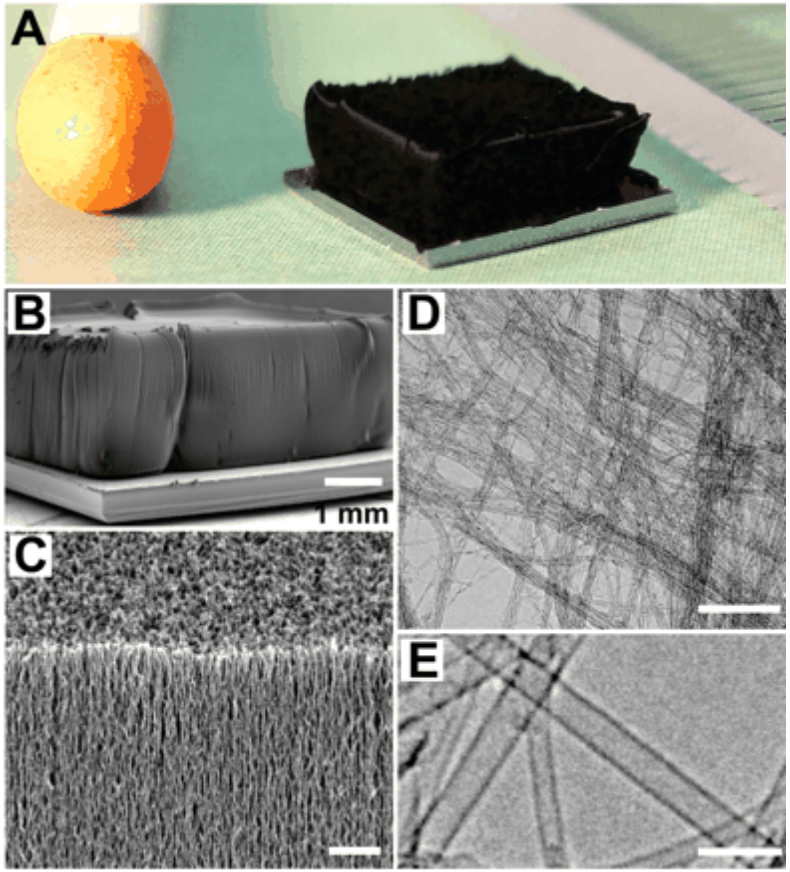

A) 2.5 mm talk SWNT "Forest"

B) SEM photograph of (A)

C) SEM of forest ledge, scale bar = 1 μm

D) Low resolution TEM, scale bar = 100 nm

E) High Resolution TEM, scale bar = 5 nm

Hata et al., Science 396, 1362 (2004)

SWNTs – Patterned Catalyst

- Can **pattern catalysts on substrate and grow SWNTs**

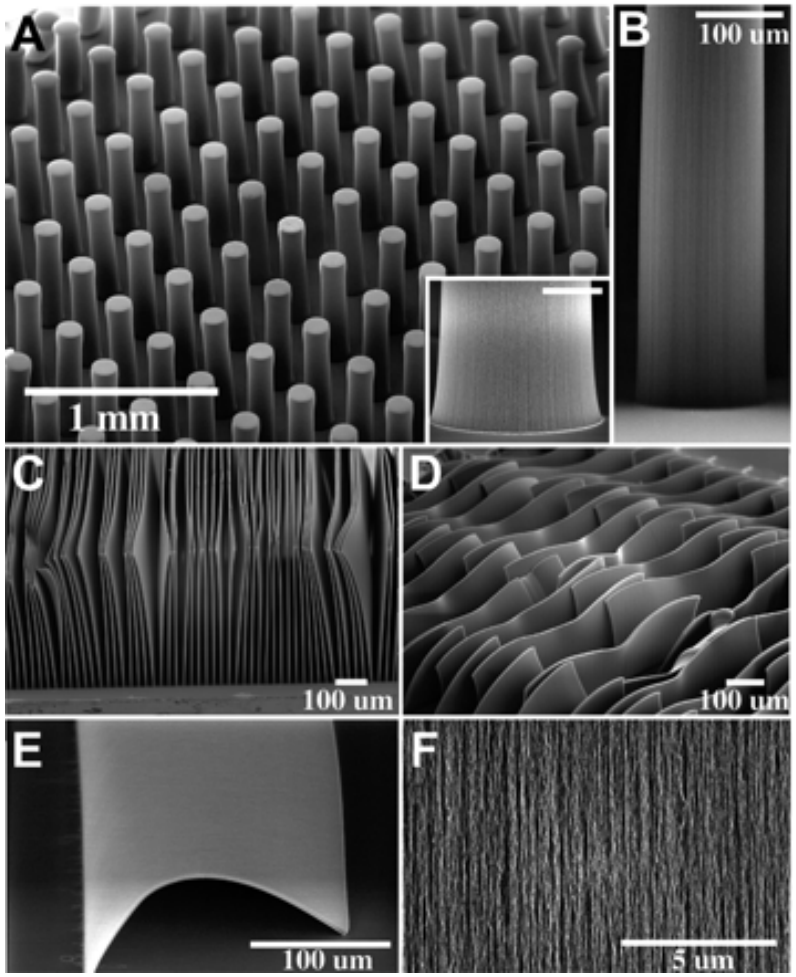

Hata et al., Science 396, 1362 (2004)

A) SEM image of SWNT cylindrical pillars with 150 μm radius, 250 μm pitch, 1 mm height

B) Side view of pillar, scale bar = 1 μm

C) SEM image of SWNT sheets

D) SWNT sheets

E) SEM image of an isolate SWNT sheet 5 μm thick

F) SEM image of sheet face

Controllability?

Despite all these different ways to create SWNTs, there's simply no way to make only metallic or semiconducting SWNTs!

Metallic

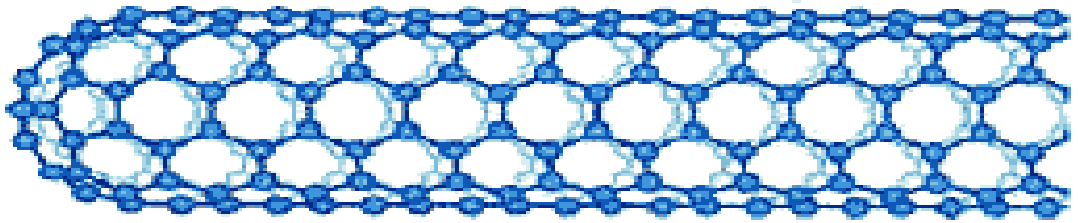

Armchair ($\alpha = 30°$)

Semiconducting/
Metallic

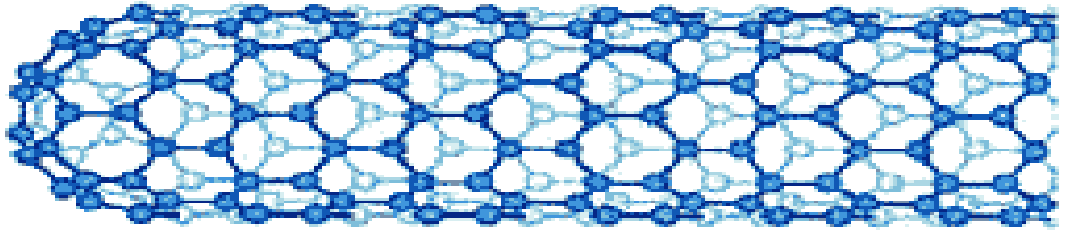

Zigzag ($\alpha = 0°$)

Semiconducting
Semimetallic

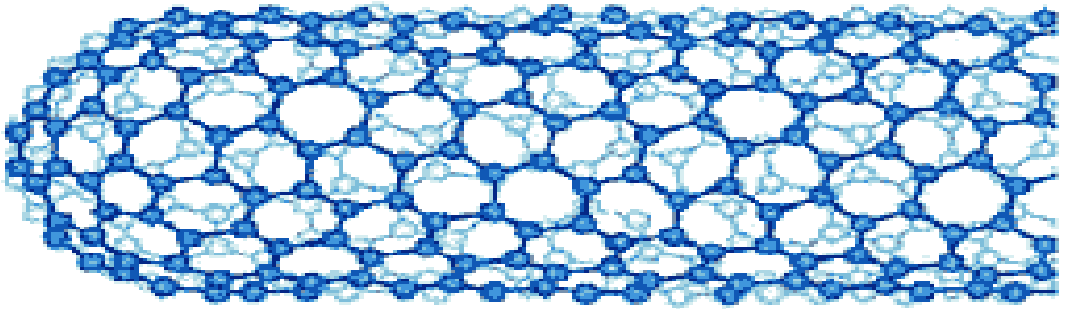

Intermediate ($0 < \alpha < 30°$)

Separate Carbon Nanotubes?

- Even though one can grow SWNTs very well, there still remains the issue of the batch of **SWNTs being metallic, or semiconducting**
- ***What to do?***

—"**Brute Force**" way: make a bunch of leads, "sprinkle" the nanotubes onto wafer, test leads

—**Dielectrophoresis** which will at least **separate metallic from semiconducting** tubes

Dielectrophoretic Separation of Nanotubes

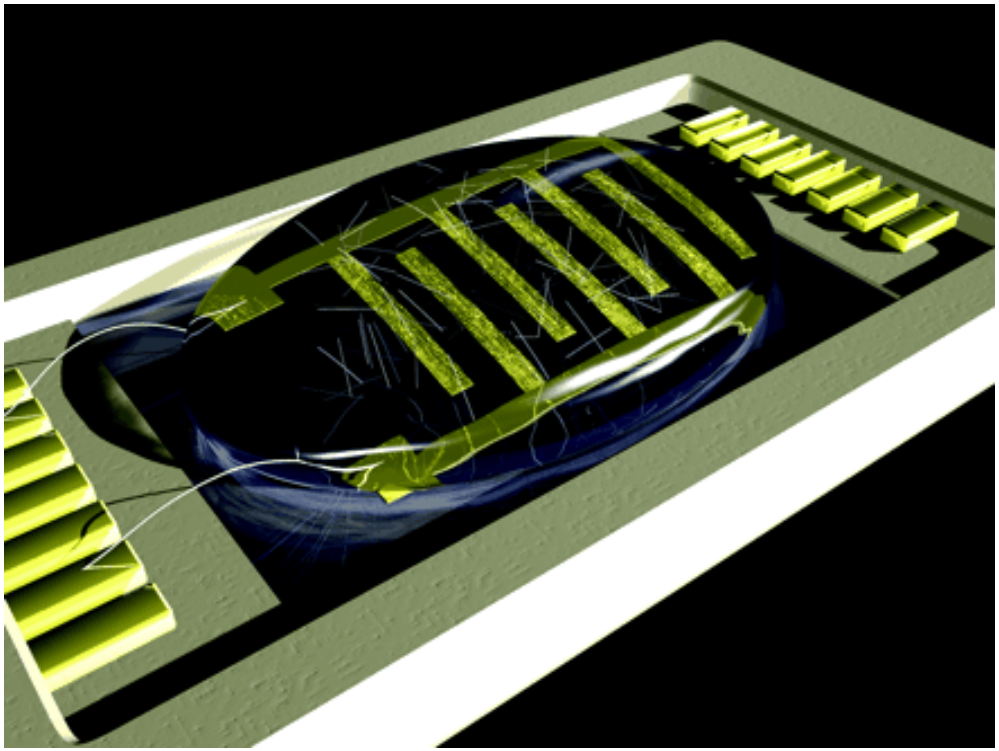

Krupke et al., Science 301, 344 (2003)

- Patterned microelectrodes with a droplet of SWNTS in solution on top
- **AC electric field** of 10 MHz, Vpp = 10 V applied for 10 min
- Drop blown off using dry nitrogen

Dielectrophoretic Separation of Nanotubes

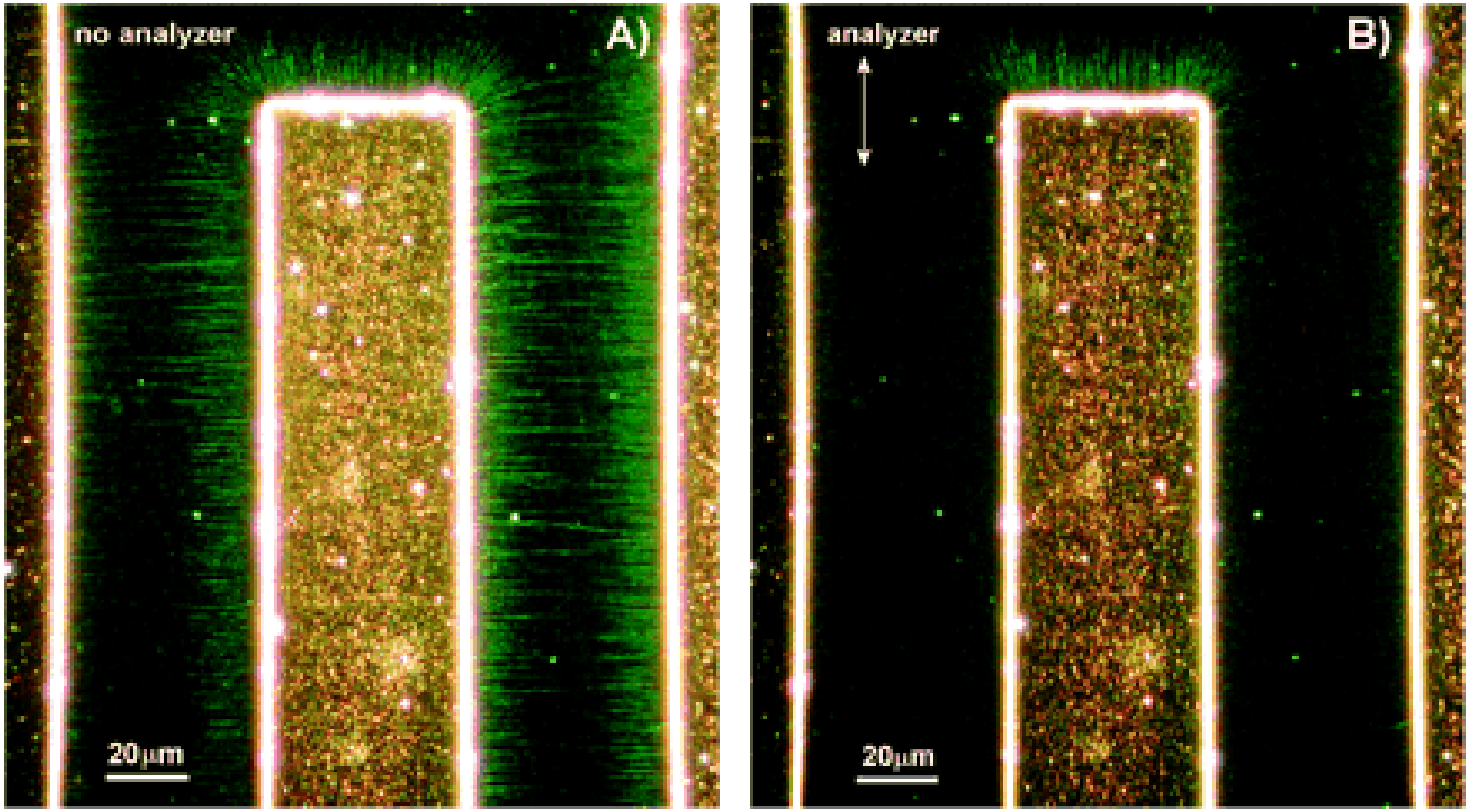

- Semiconducting SWNTs remain in suspension but metallic ones deposited onto electrodes
- Krupke et al. estimate that 80% are metallic

CNT Fabrication - Summary

- Discussed a variety of ways to **synthesize CNTs**
  - DC arc discharge
  - Pulsed-laser ablation
  - Chemical vapor deposition
- Also, discussed methods to **separate CNTs**
  - Dielectrophoresis


Carbon Nanotube
Growth by CVD Method
Qin Zhou

Method Overview

- 1. Select a substrate
- 2. Form catalyst particle (Fe, Co, etc.)
- 3. Put into furnace
- 4. Flow gas
- 5. Raise temperature
- 6. Keep temperature
- 7. Cool down

Growth Condition

- Substrate
  - -Silicon dioxide
  - -Other oxides
  - -Metal
- Catalyst Particle
  - -Determine the diameter of CNT
  - -Evaporation
  - -Solution
- Gas
- Temperature

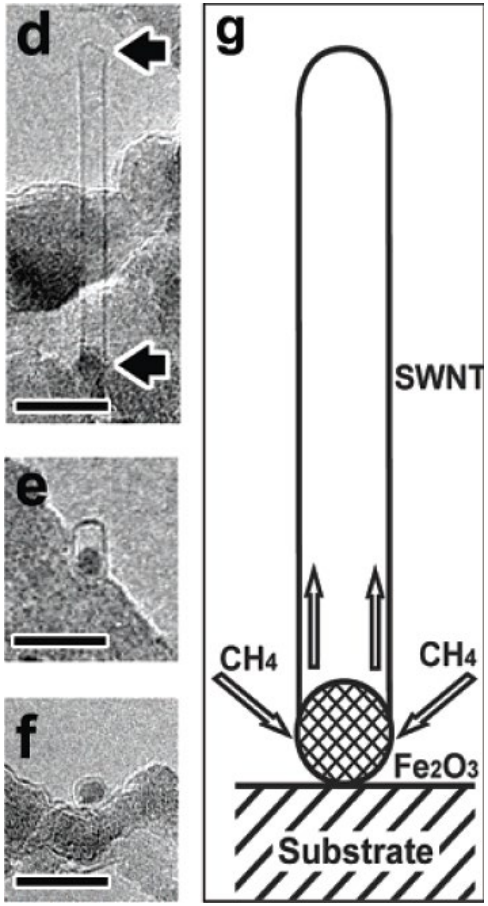

Dai, H. et al. Acc. Chem. Res. 35, 1035

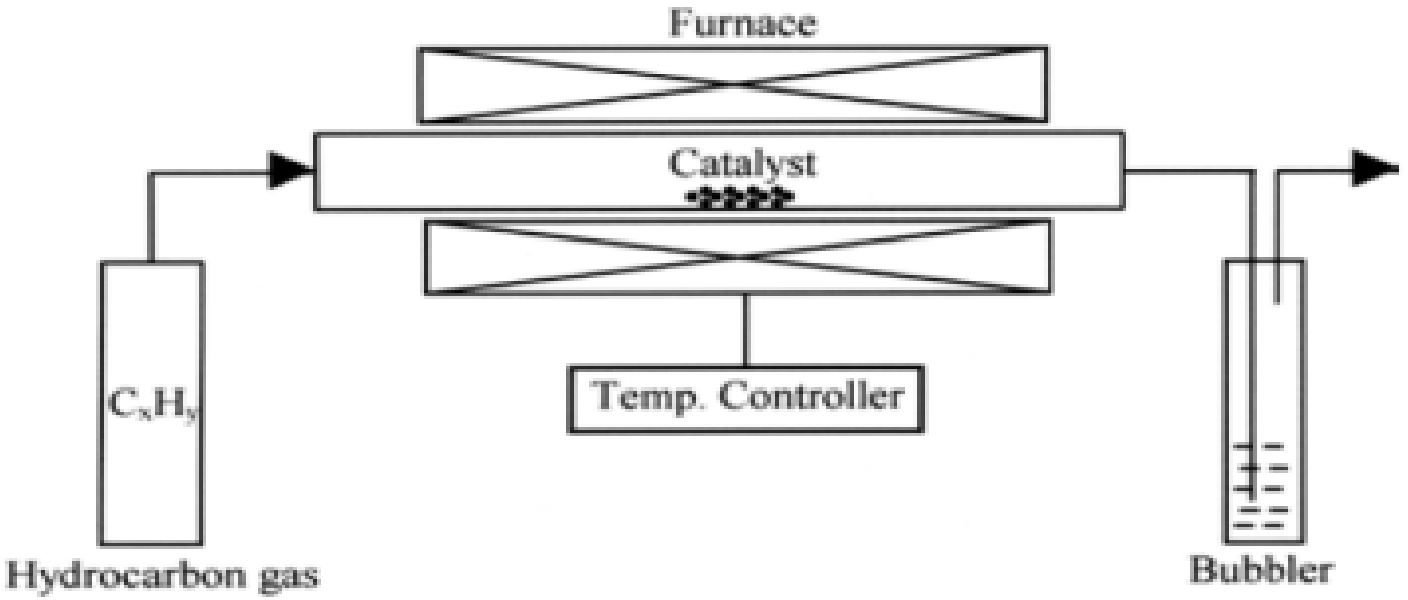
Furnace
Catalyst
Temp. Controller
C_xH_y
Hydrocarbon gas
Bubbler

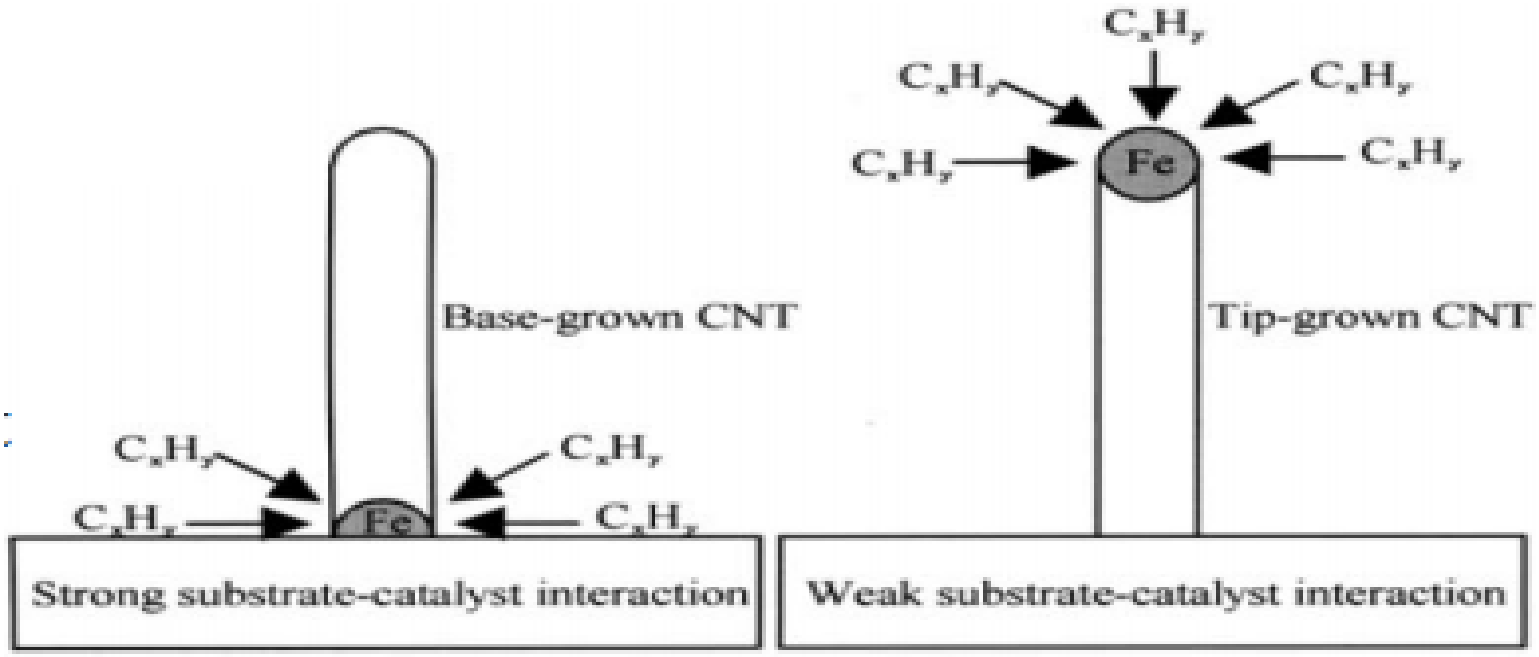
C_xH_y
C_xH_y
C_xH_y
C_xH_y
C_xH_y
Fe
Base-grown CNT
Tip-grown CNT
C_xH_y
C_xH_y
C_xH_y
C_xH_y
Fe
Strong substrate-catalyst interaction
Weak substrate-catalyst interaction

Typical Process Description

- Forming catalyst on substrate

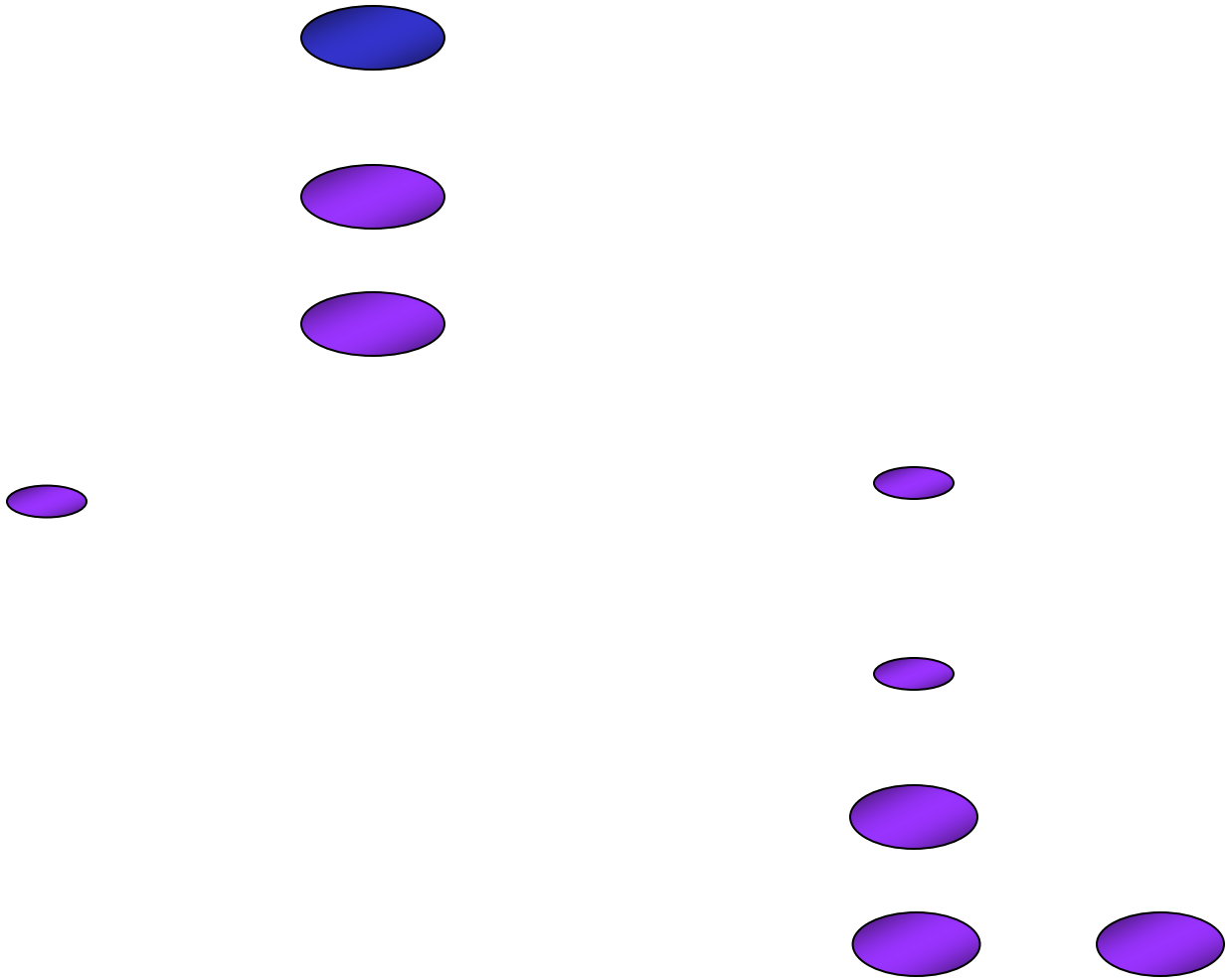

Growth Result

- SEM can be used to have an overview of the whole substrate

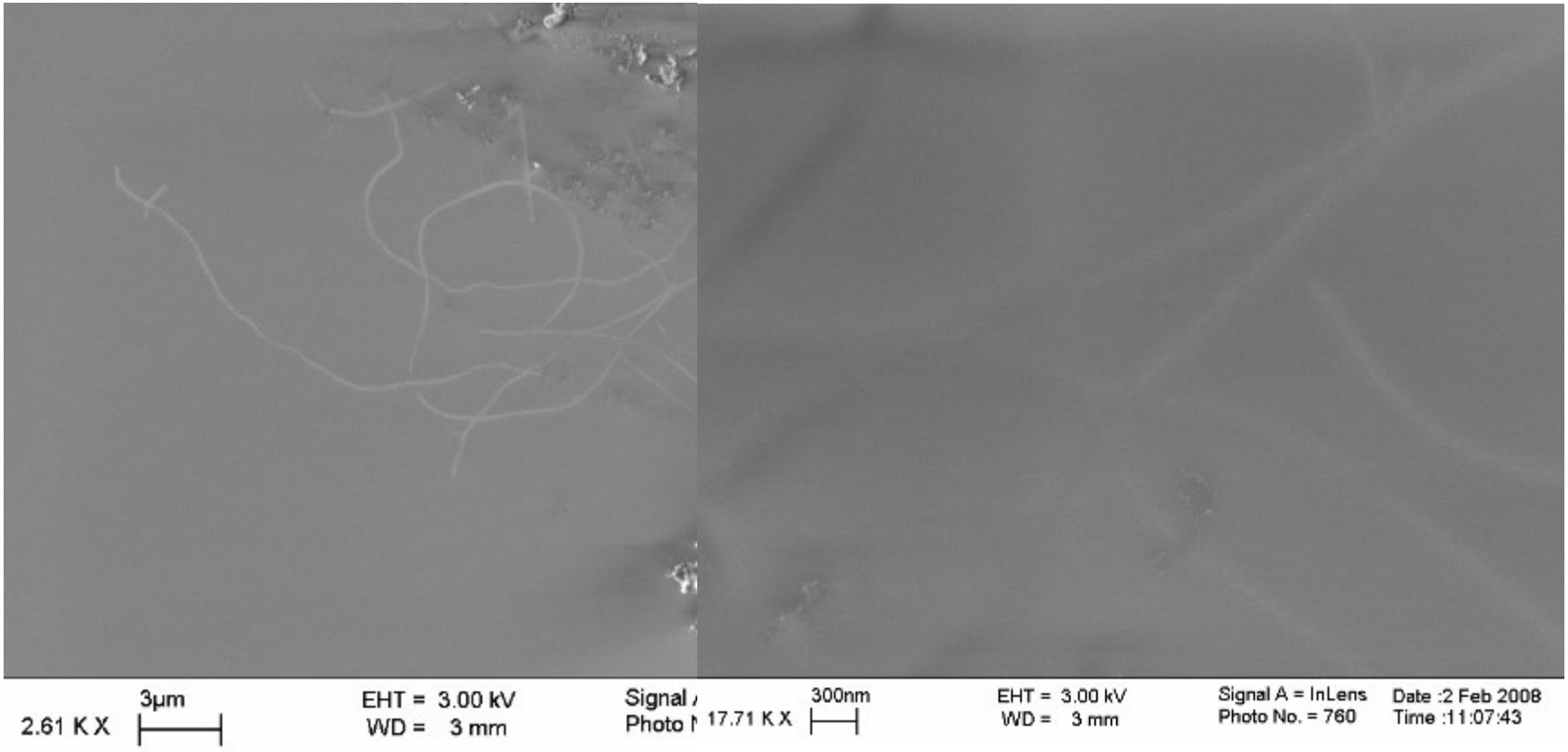

Growth Result

- AFM can get a much clearer image, and it can also perform measurement on the dimension of CNT

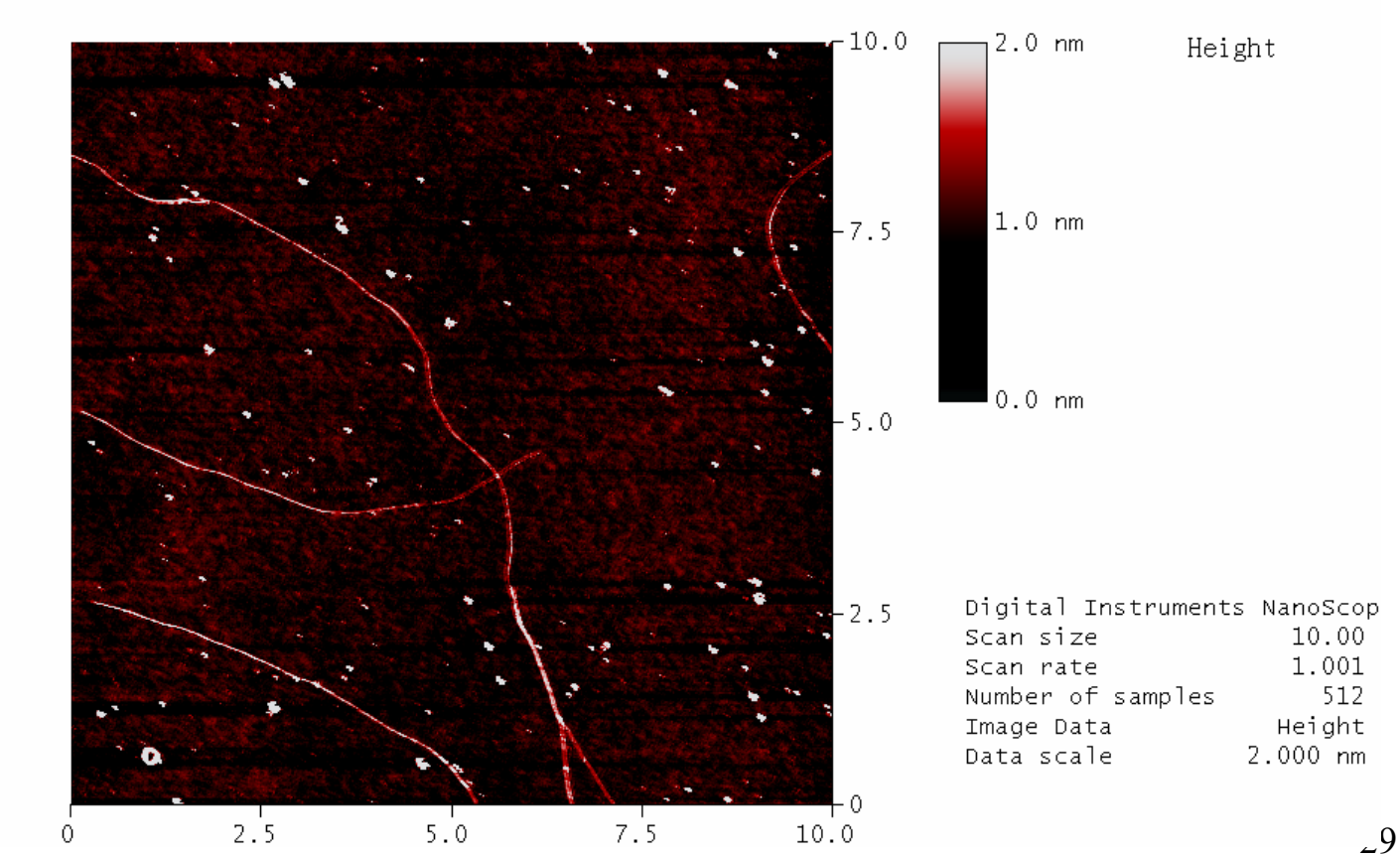

Resonator Frequency

- Resonator Frequency: spring-mass

$$f = \frac{1}{2\pi}\sqrt{\frac{k}{m}}$$

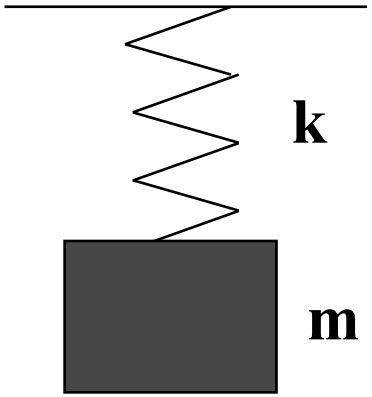

- Clamped-Clamped beam

$$k = \frac{192EI}{L^3}$$

Cantilever Example

- Resonant frequency ($k \sim 10^{-3} - 10^{0}$ N/m)

$$f_0 = \frac{1}{2\pi}\sqrt{\frac{k}{m}} \qquad k = \frac{3EI}{l^3}$$

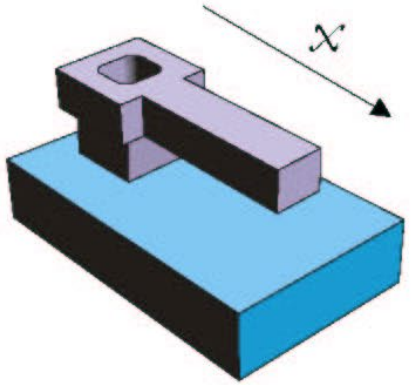

$$f_0 \longrightarrow \frac{t}{4\pi l^2}\sqrt{\frac{E}{\rho}}$$

–MEMS cantilever $100 \times 3 \times 0.1$ μm³, f_0=12 kHz

–NEMS cantilever $0.1 \times 0.01 \times 0.01$ μm³, f_0=1.2 GHz

Quality Factor

- "Q" gives you an idea on damping - total energy stored/total energy lost per cycle
- if the cantilever strongly [weakly] damped, then the Q will be low [high]
- what determines Q
  - material (Si_3N_4, polysilicon, single crystal Si)
  - geometry
  - surface treatments
  - environment (vacuum, liquid, temperature)

HW#3

University of California at Berkeley
College of Engineering
Mechanical Engineering Department

ME118/218N, Spring 2024 **Liwei Lin**

Problem Set #3
Due Feb. 15 (Thursday)

Problem 1 (CNT Fabrication)

Describe two methods of making carbon nanotubes? You may "google" the methods to help summarizing your descriptions. Please limit yourself to no more than 0.5-page per description and draw a simple figure to illustrate each method.

HW#3

Problem 2 (CNT Resonator)

A carbon nanotube is suspended between two contacts as shown below (W in the figure is 1.0 μm. Figure is from Sazonova et al., *Nature* **431**, 284 - 287 2004)

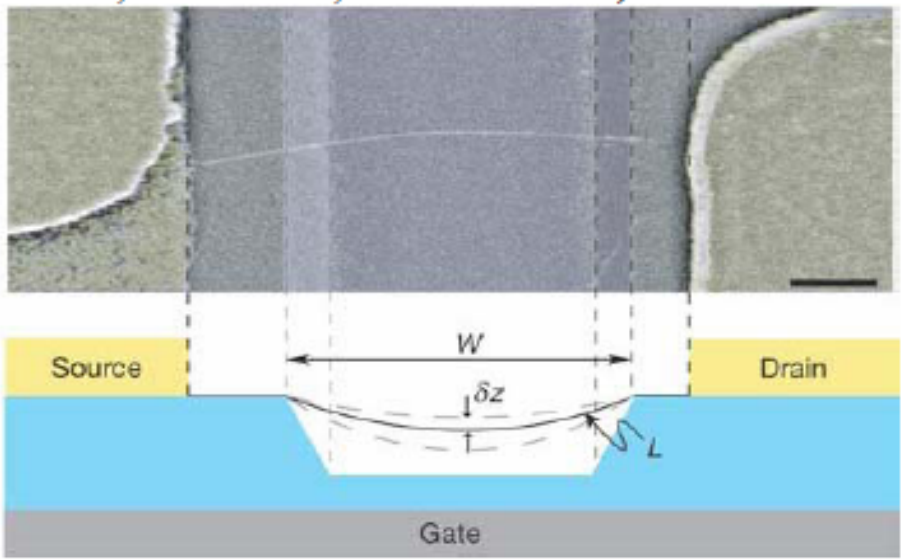

(a) design a process flow to make this set up (you can either come up your own process or take a look at the original paper to see how they did it)

(b) What is the mechanical resonance frequency of the nanotube? Consider that the diameter, D, of the carbon nanotube is 1.3 nm, the length, and the Young's Modulus, E, is 1.2 TPa. You will need to know that the moment of the cross-sectional area of the carbon nanotube about the neutral axis is $I = (\pi d^4/64)$

(c) Compare this resonance frequency with that of one suspended single-crystal silicon beam that is 7.7μm in length, 330nm in width, and 800nm in height.

(d) What do the first four resonance modes of the suspended carbon nanotube look like? Sketch a drawing of these modes.

HW#3

Problem 3 (CNT Applications)

We discussed one possible sensing application for CNT in paper 3. You are asked to search and find two other potential applications for (1) CNT sensors, (2) CNT applications in biomedical areas. Please limit yourself to no more than 0.5-page per application and draw a simple figure to illustrate each application and state WHY CNT would be an excellent candidate for that particular application.

Laser-induced porous graphene films from commercial polymers

Jian Lin1,2, Zhiwei Peng3, Yuanyue Liu1 , Francisco Ruiz-Zepeda4, Ruquan Ye3, Errol L.G. Samuel3, Miguel Jose Yacaman4, Boris I. Yakobson1,2,3 & James M. Tour1,2,3

Over the past decade

Graphene-based nanomaterials have been widely studied due to their unique properties.

Graphene can be engineered to possess porous and three-dimensional (3D) structures.

The goal is to address the technological gap by achieving a straightforward synthesis of graphene-based nanomaterials for a microscale energy storage devices.

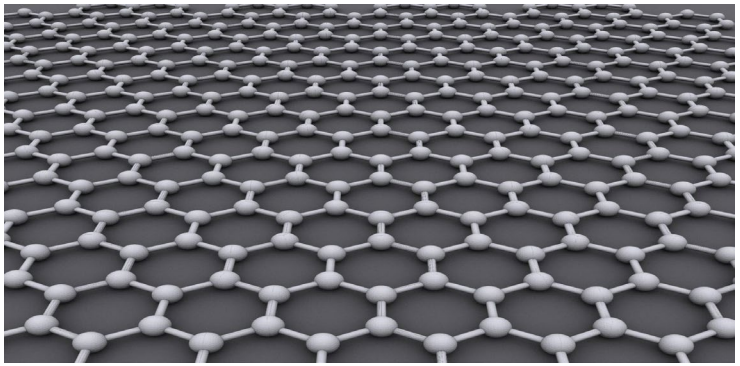

Figure 1: shows Graphene polymers

Review about this method

This study demonstrates the production of 3D porous films from polymers from laser induction.

Why Laser Induction?

It offers a simple and an efficient way to transform regular polymers into graphene structures.

Subjecting some polymer films to a CO_2 infrared laser irradiation to transform it into the desired 3D porous graphene structure.

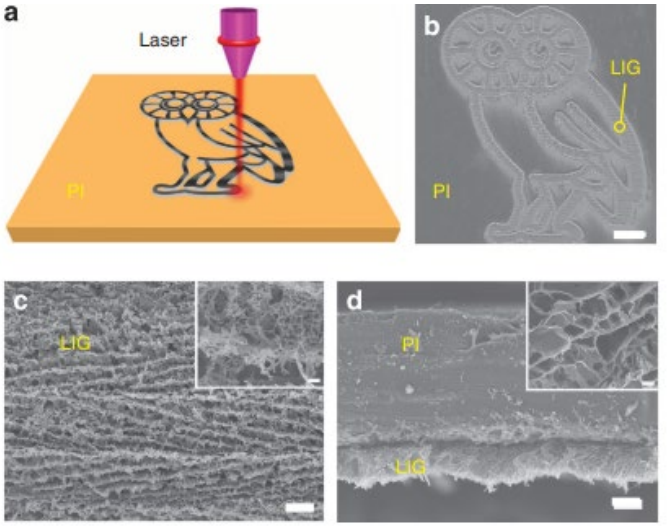

Figure 2: CO2 Laser-Patterned LIG from Commercial PI Films at 3.6W Jian Lin 2014

Benefits of this method

Cost-Effective as it uses readily available plastic films which reduces the material costs.

It is a one step technique which enables rapid and continuous production which allows for roll-to-roll manufacturing

Can be easily patterned into specific shapes, opening doors for diverse applications

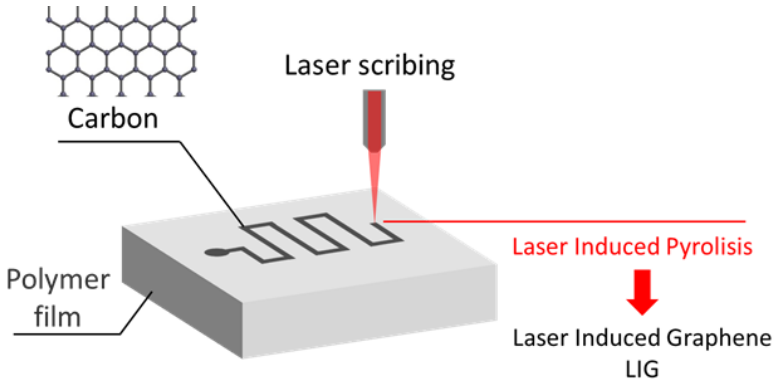

Figure 2: polymer to graphene transformation via laser Lin Juan Laser- induced porous graphene films from commercial polymers 2014

Future applications

Fu Liu have reported a new method which is called laser-induced graphene additive manufacturing.

This method allows for the creation of bulk 3D graphene structures without the need for additional binders or catalysts.

Precisely control LIG-AM with laser power and powder thickness; proven success in smart device printing

https://www.sciencedirect.com/science/article/abs/pii/S1369702123003383?via%3Dihub

RESULTS

Ahmed alhosani

AHMED ALHOSANI

RESULTS

- LASER SCRIBING
- ANALYTICAL CHARACTERIZATION
- EFFECT OF LASER POWER
- TEM IMAGES
- SUMMARY

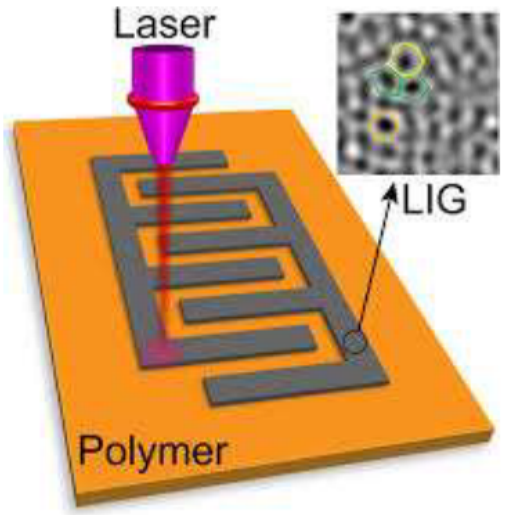

LASER SCRIBING

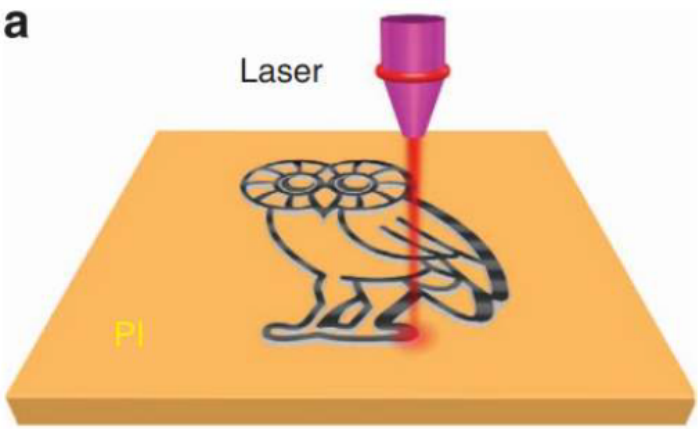

- When pulsed laser radiation is applied, the sp3-carbon atoms photothermally transform into sp2-carbon atoms.
- High electrical conductivity is displayed by the resulting laser-induced graphene (LIG).

3

ANALYTICAL CHARACTERIZATION

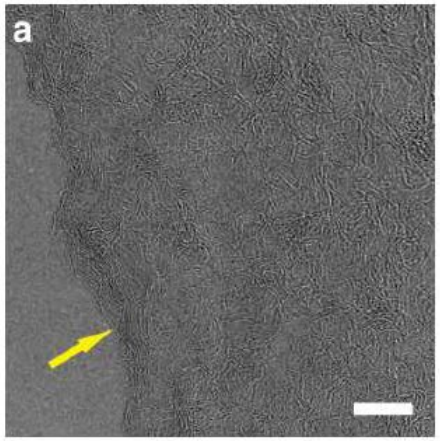

The Raman spectra that result from carbonizing PI at temperatures between 800 and 1,500 C is comparable to that of glassy carbon (Supplementary Fig. a). However, the LIG (Fig. 1d) spectrum differs from the glassy carbon spectra.

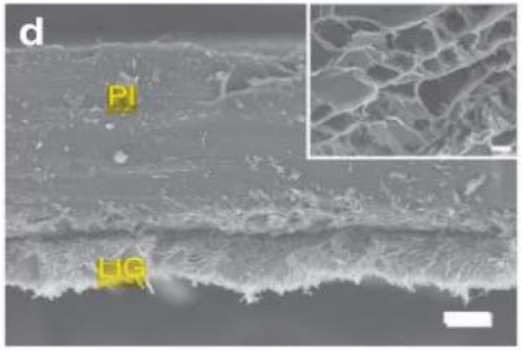

LASER IMPACT

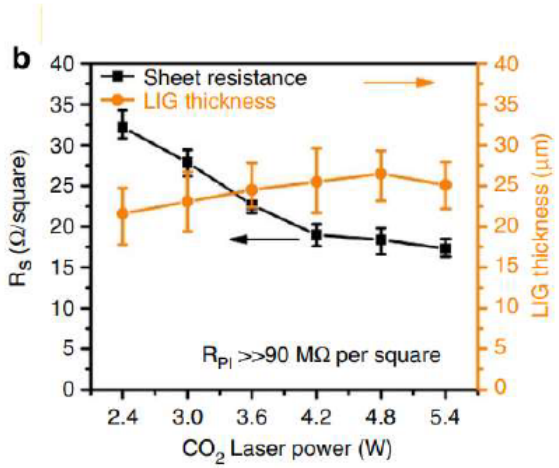

LIG was created with powers ranging from 2.4 W to 5.4 W in 0.6 W increases at a scan rate of 3.5 inches per second to examine the impact of laser power.

As a result, enhancing laser power corresponds to higher graphitization levels. Oxidation begins to adversely affect the film quality when the thermal power increases above 4.2 W. As a result, the slope decreases.

5

TEM IMAGES

RAMAN SPECTRUM IS REPRESENTATIVE OF THE INITIAL PI FILM AND A LIG FILM.

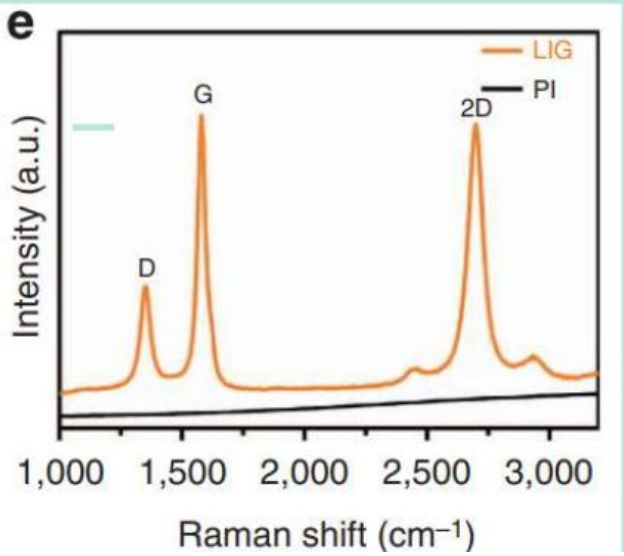

IT DISPLAYS A HEXAGON WITH A SCALE BAR OF 5 AND A HEPTAGON WITH TWO P

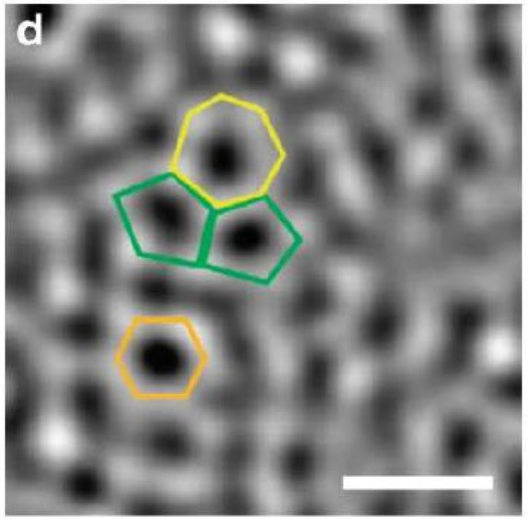

SUMMARY

- The resulting LIG structures' unique combination of chemical and physical characteristics make them ideal for energy storage devices with promising electrochemical performance.
- Roll-to-roll production, a sign of easy commercialization, might be achieved with the application of commercially accessible polymer sheets.
- There is a versatile, one-step method for producing porous graphene from commercial polymer sheets by irradiating them with a CO_2 laser in ambient environments.

Laser-Induced Graphene Formation

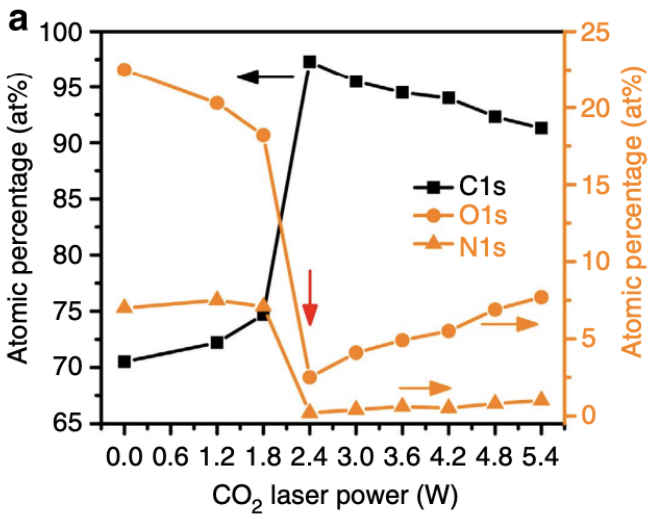

Fig. 3(a) Atomic percentages of carbon, oxygen and nitrogen as a function of laser power. These values are obtained from high-resolution XPS. The threshold power is 2.4W, at which conversion from PI to LIG occurs

- The energy from the laser leads to extremely high localized temperatures (> 2500 °C).
- This high temperature breaks specific bonds (C – O, C = O and N – C bonds) and causes subsequent release of gases.
- Aromatic compounds rearrange to form graphitic structures, with an overlayer of evolved gases minimizing oxidation.
- The mechanism of laser graphitization is linked to structural features in polymer repeat units, especially aromatic and imide units. Only 2 out of 15 tested polymers can form LIG. They both contain aromatic and imide repeat units.

Jason

In-Plane Interdigitated LIG Microsupercapacitors (LIG-MSCs)

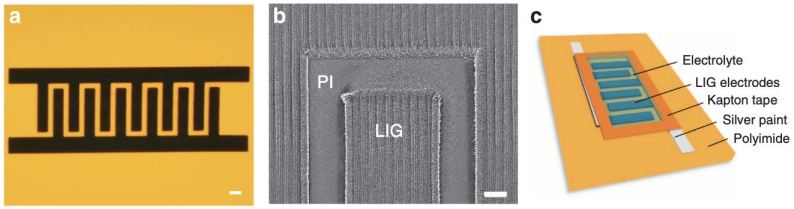

Fig. 4(a) A digital photograph of LIG-MSCs with 12 interdigital electrodes; scale bar, 1 mm.

Fig. 4(b) SEM image of LIG electrodes; scale bar, 200 mm.

Fig. 4(c) Schematic diagram of LIG-MSCs device architecture.

- LIG serves as both the active electrodes and the current collectors.
- Well-defined LIG-MSC electrodes are directly written on PI sheets with a neighbouring distance of 300 μm
- Silver paint was applied on common positive and negative electrodes.
- Kapton tape was employed to define the active electrodes.

Jason

Electrochemical Performance

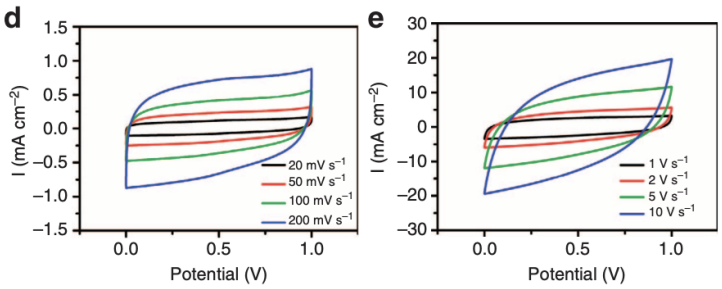

4(d & e) CV curves of LIG-MSCs at scan rates from 20 to 10000 mVs^{-1}

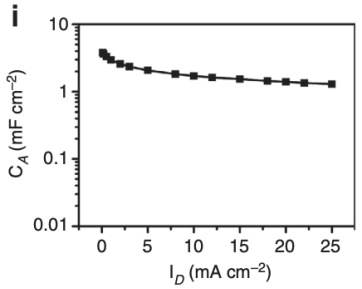

4(f) Specific areal capacitance (C_A) calculated from CV curves as a function of scan rates

Jason

- Cyclic voltammetry (CV) and galvanostatic charge – discharge (CC) measurements were performed to investigate the electrochemical performance of the fabricated LIG-MSCs
- Good double-layer capacitive behaviours are shown from the CV curves.
- LIG-MSCs constructed with LIG-4.8 W electrodes exhibit the highest specific areal capacitance.
- All other electrochemical measurements were carried out on LIG-MSCs made from PI with a laser power of 4.8 W.

Electrochemical Performance

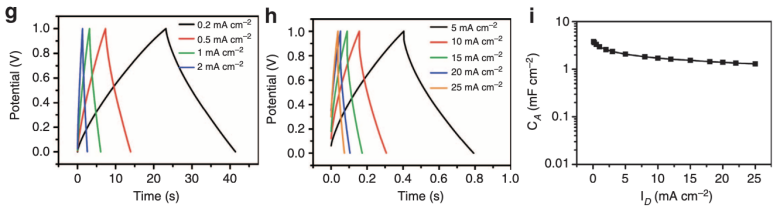

Fig. 4(g & h) CC curves of LIG-MSCs at discharge current densities (I_D) varied from 0.2 to 25 mA cm^{-2}.

Fig. (I), C_A calculated from CC curves versus I_D

- After comparing capacitance with GO-derived supercapacitors and carbon-based MSCs, LIG-MSCs show excellent capacitive behaviour.
- A low equivalent series resistance of 7 Ω suggests good conductivity and rapid charge-discharge capabilities.

Jason

Electrochemical Performance

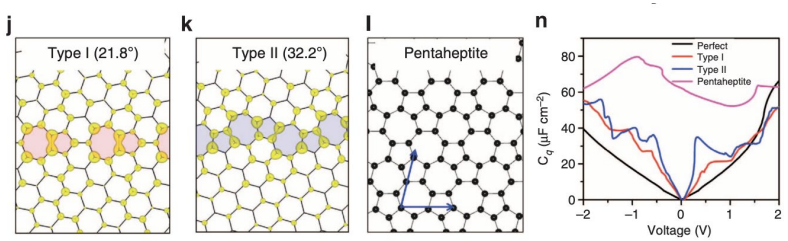

Fig. (j and k), Charge density distribution of the states within a voltage window (-0.1, 0.1) V for type I and II polycrystalline sheets. The defects at the grain boundaries are shadowed, and numbers show the misorientation angle between the grains.

Fig. (l) A carbon layer fully composed of pentagons and heptagons (pentaheptite).

Fig. (n) Calculated quantum capacitance (defined in the text) of perfect and polycrystalline/disordered graphene layers.

- LIG-MSCs offer more energy or power density or both.
- When compared with recently demonstrated reduced GO-film, MSCs (MPG-MSCs), and laser-scribed graphene MSCs (LSG-MSCs), LIG-MSCs can deliver comparable E_V, although power performance needs to be enhanced.
- LIG-MSCs exhibit 100 times higher areal energies E_A and 4 times power densities P_A than MPG-MSCs.
- LIG-MSCs offer slightly better E_A than LSG-MSCs with comparable power performance.

Jason

Methods

Experimental Setup

- Utilized Kapton Polyimide film and various polymer sheets from McMaster-Carr
- CO_2 laser cutter system (Universal X-660) with 10.6 mm wavelength and 14 ms pulse duration employed for laser scribing.
- Laser power varied from 2.4 to 5.4W with 0.6W increments; fixed scan rate of 3.5 inches/s and 1,000 pulses per inch.

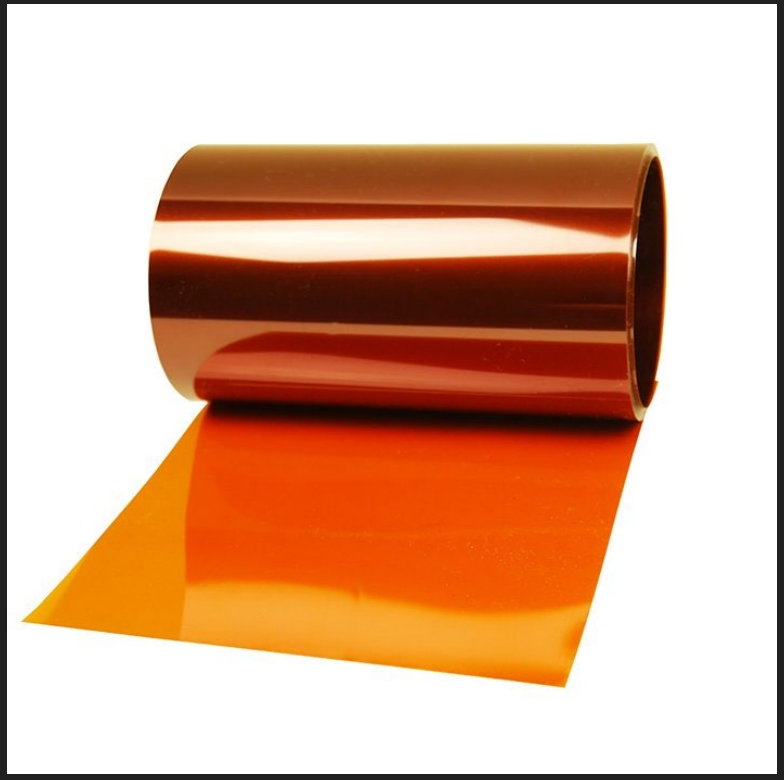

Methods

Methodological Parameters

- Laser system options included adjustable scan rates (0.7 to 23.1 inches/s) and p.p.i. settings (10–1,000 p.p.i.).
- Experimentation revealed pulses per inch (ppi) had minimal impact on changing threshold power.
- All laser experiments conducted under ambient conditions had consistent scan rate (3.5 inches/s) and 1,000 p.p.i. was used for all experiments unless specified otherwise.

Methods

Device Fabrication Overview

- CO_2 laser used for direct writing of LIG electrodes.
- Laser-Induced Graphene serves as active electrodes and current collectors in microsupercapacitors.
- Silver paint enhances electrical connectivity; Kapton PI tape protects contact pads in the meshed area.

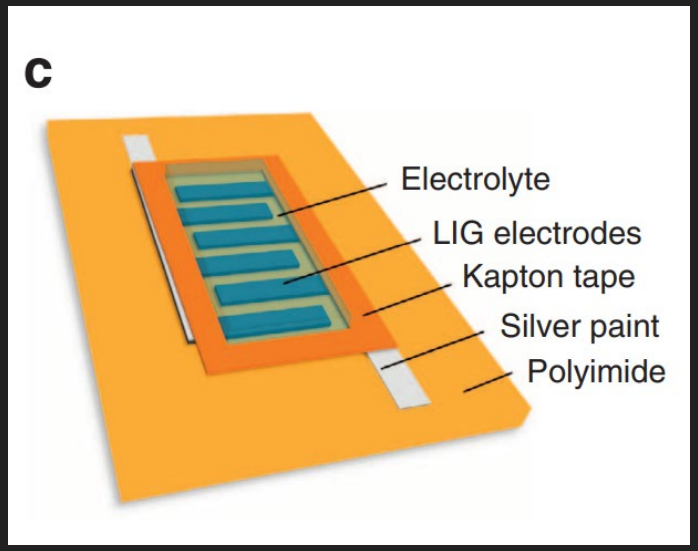

Methods

Characterization

- SEM images were taken on a FEI Quanta 400 high resolution field emission instrument.
- The TEM and high-resolution TEM were performed using a 2,100 F field emission gun.
- Aberration-corrected scanning TEM images were taken using an 80 kiloelectron volt Japan Electron Optics Laboratory ARM200F equipped with a spherical aberration corrector.

Methods

Measurements

- CV, galvanostatic CC measurements, and electrical impedance testing performed using a CHI 608D workstation.

- All measurements conducted in ambient conditions.

- The experimental focus extended to include aqueous electrolytes.

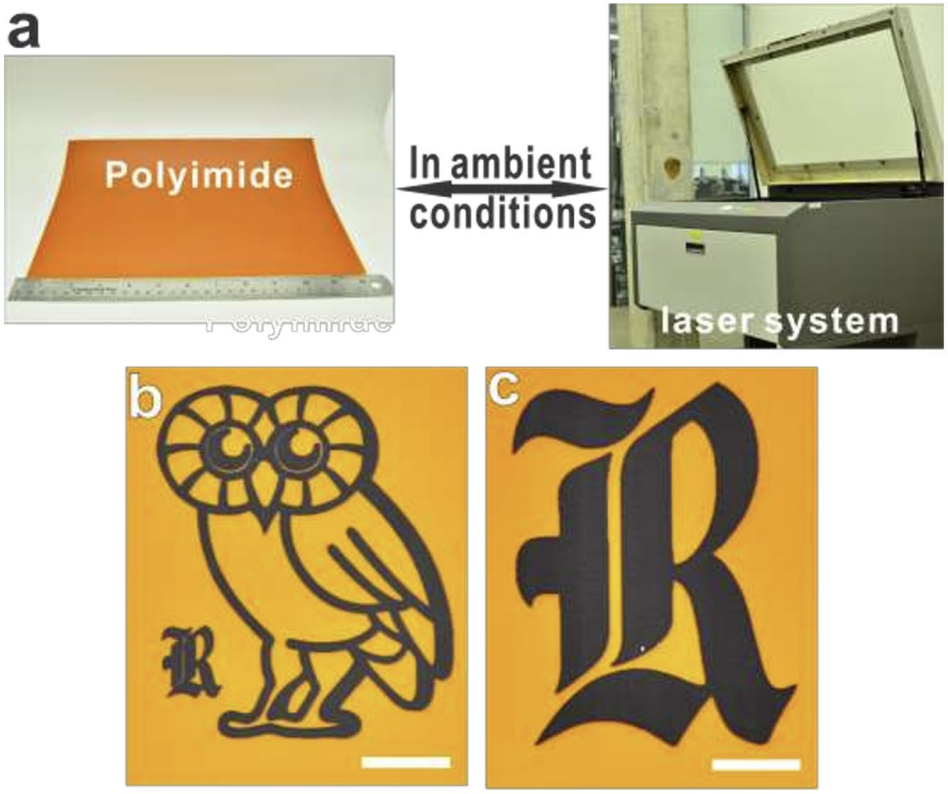

Materials and equipment for production of LIG from PI by laser scribing

a) Photographs of commercial Kapton PI sheets with a 30 cm ruler on the left, and the laser cutting system on the right
b) Photograph of an owl patterned on a PI substrates;
c) Photograph a letter R patterned on a PI substrate;

Transmission Electron Microscopy (TEM) Characteristics of LIG-3.6 w Flakes

a) TEM image of a thin LIG flake atop a carbon grid; scale bar 200 nm
b) TEM image of a thick LIG flake showing entangled tree-like ripples; scale bar 100 nm
c) TEM image of LIG in bright field view; scale bar 10 nm
d) TEM image of LIG in dark field view; scale bar 10 nm

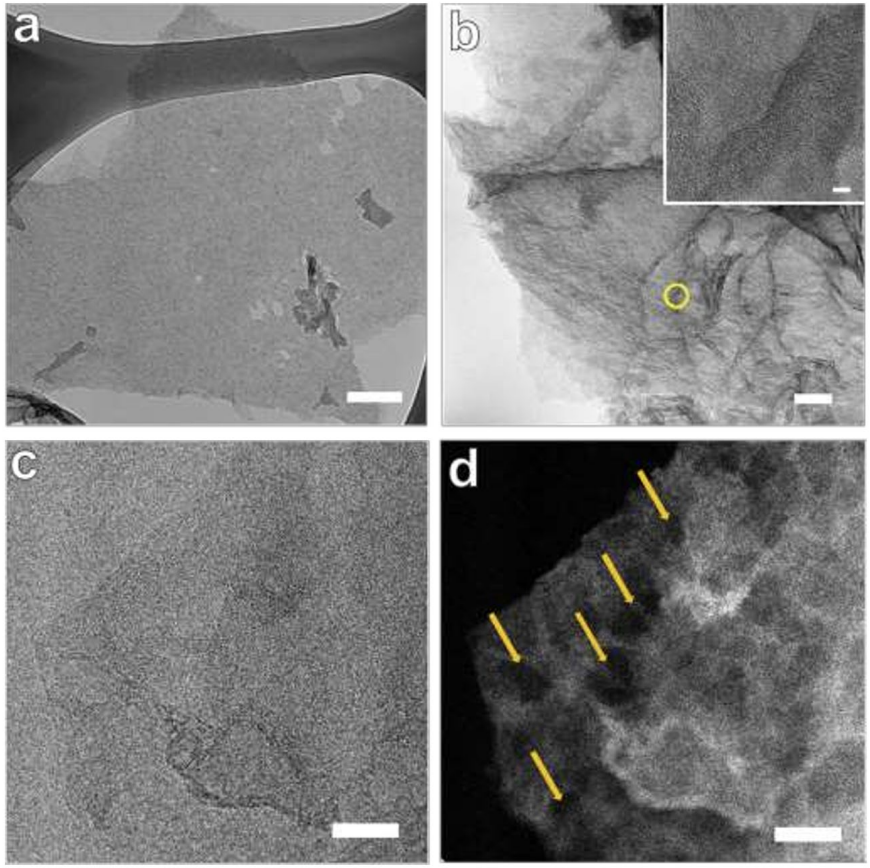

Characterizations of backsides of LIG films

a) Scheme of the backsides of LIG films peeled from PI substrates.
b) SEM images of backsides of LIG films obtained at laser powers of b) 2.4 W; c) 3.6 W; and d) 4.8 W; Scale bars are 10 nm

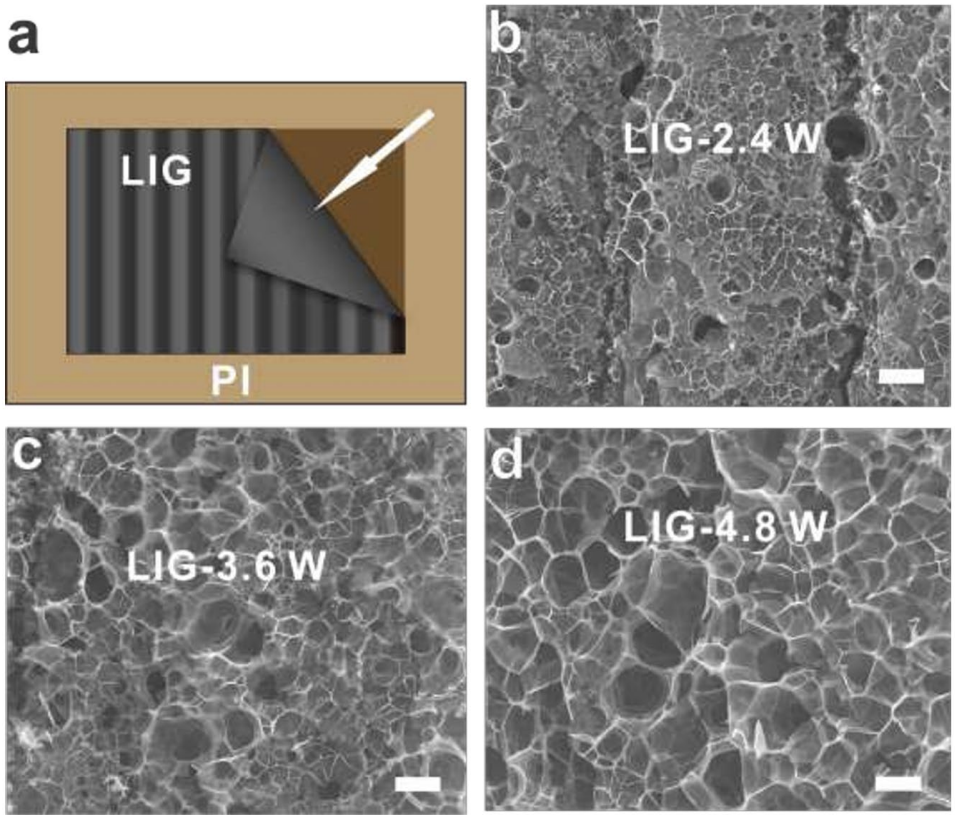

Supplementary Tables

Summary of polymers, their chemical repeat units and their LIG forming capability. Out of 15 polymers, only PI and PEI were successfully converted to LIG.

Full Name	Symbols	Unit	Graphitized?
Kapton Polyimide	PI		Yes
Ulse Polyetherimide	PEI	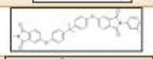	Yes
Polyether ether ketone	PEEK	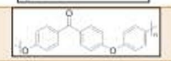	No
Polyethylene terephthalate	PET	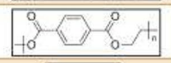	No
Polyethylene naphthalate	PEN		No
Fluorinated ethylene propylene	FEP		No
Perfluoroalkoxy alkanes	PFA		No
Teflon	PTFE		No
Polystyrene	PS		No
Polycarbonate	PC	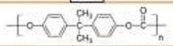	No
Polyethylene	PE	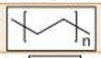	No
Polyvinyl alcohol	PVA		No
Poly(methyl methacrylate)	PMMA		No
Acrylonitrile butadiene styrene	ABS		No
Poly(acrylonitrile)	PAN		No

Materials	Carbon (%)	Oxygen (%)	Nitrogen (%)
Polyimide	70.5	22.5	7.0
LIG-1.2 W	72.2	20.3	7.5
LIG-1.8 W	74.7	18.2	7.1
LIG-2.4 W	97.3	2.5	0.2
LIG-3.0 W	95.5	4.1	0.4
LIG-3.6 W	94.5	4.9	0.6
LIG-4.2 W	94.0	5.5	0.5
LIG-4.8 W	92.3	6.9	0.8
LIG-5.4 W	91.3	7.7	1.0

Summary of atomic percentage of elements in raw material (PI) and LIG derived from different laser powers.

Fabrication process of LIG microsupercapacitor

It took ~15 min to fabricate these devices with ~7 cm × ~6 cm area. This movie shows that this technology in fabricating in-plane supercapacitors can be easily scaled.

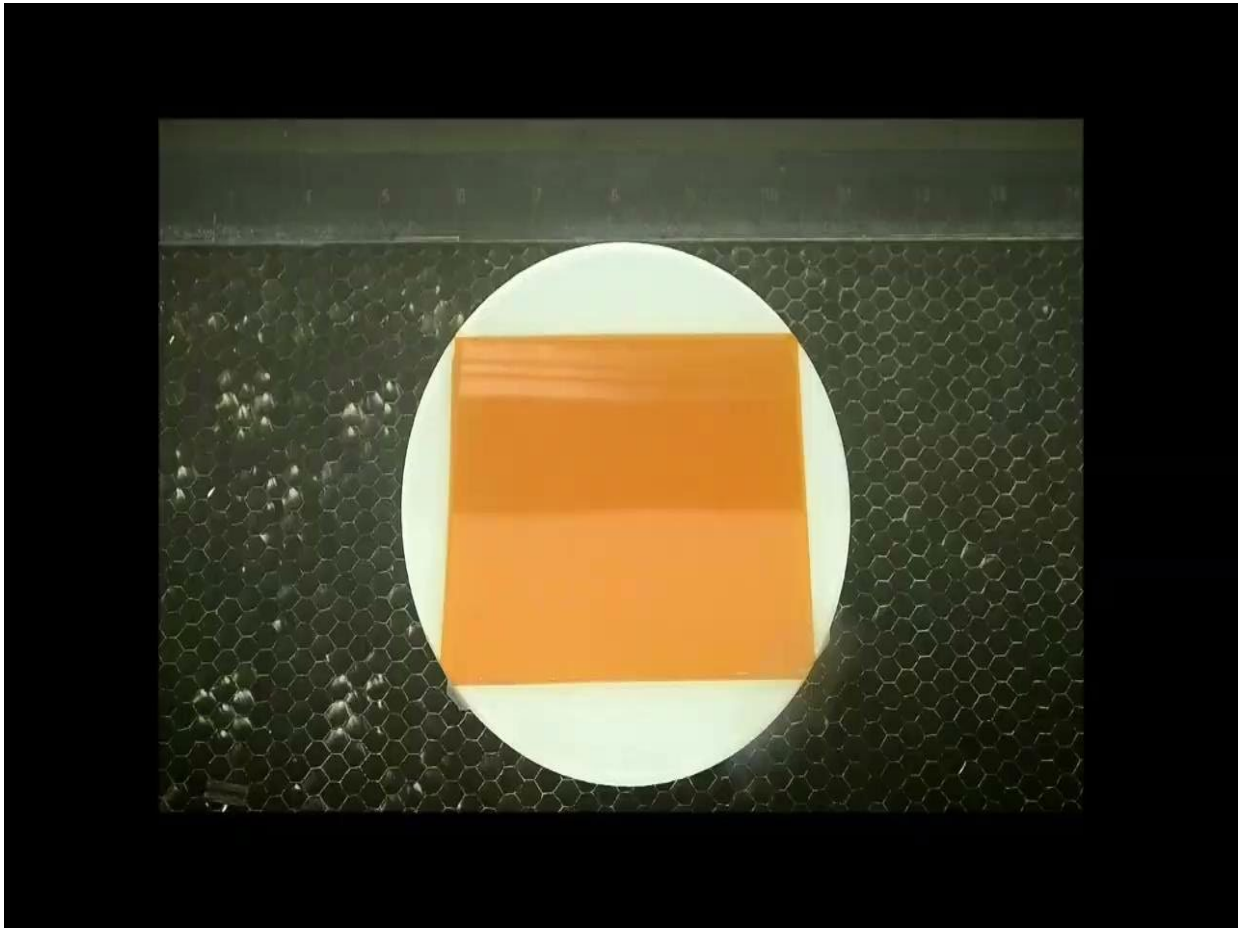

References

1. Lin, J., Peng, Z., Liu, Y., Ruiz-Zepeda, F., Ye, R., Samuel, E. L. G., Yacamán, M. J., Yakobson, B. I., & Tour, J. M. (2014). Laser-induced porous graphene films from commercial polymers. *Nature Communications*, *5*(1). https://doi.org/10.1038/ncomms6714
2. Ma, J., Alfe, D., Michaelides, A. & Wang, E. Stone-Wales defects in graphene and other planar sp(2)-bonded materials. Phys. Rev. B 80 (2009).
3. El-Kady, M. F. & Kaner, R. B. Scalable fabrication of high-power graphene micro supercapacitors for flexible and on-chip energy storage. Nat. Commun. 4, 1475 (2013).
4. Wu, Z. S., Parvez, K., Feng, X. L. & Mullen, K. Graphene-based in-plane micro supercapacitors with high power and energy densities. Nat. Commun. 4, 2487 (2013).